SEMMELWEIS EGYETEM

DOKTORI ISKOLA

Ph.D. értekezések

3469.

KOVÁCS BEATRIX HELGA

Funkcionális Idegtudományok

című program

Programvezető: Dr. Sperlágh Beáta, egyetemi tanár

Témavezető: Dr. Hillier Dániel, kutatócsoport-vezető

OPTIMIZING AAV-MEDIATED NEURAL GENE THERAPY: A NEXT-GENERATION NEUTRALIZATION ASSAY FOR PATIENT STRATIFICATION

PhD thesis

Beatrix Helga Kovács

Semmelweis University Doctoral School
János Szentágothai Neurosciences Division

Supervisor: Dániel Hillier, Ph.D

Official reviewers: Amarilla Barcsay-Veres, Ph.D
Tobias Brügmann, Ph.D

Head of the Complex Examination Committee: Alán Alpár, D.Sc

Members of the Complex Examination Committee: Mirella Barboni, Ph.D
Tamás Garay, Ph.D

Budapest
2026

“- Buta vagyok én, Karak?

- Nem vagy buta, csak még keveset tudsz.”

István Fekete: Vuk

Table of Contents

List of Abbreviations

AAV	Adeno-associated virus
ADK9	Anti-AAV9 monoclonal antibody (clone ADK9)
CI	Confidence interval
CI-of-CIs	Confidence interval of credible intervals
coreTIA	Core Transduction Inhibition Assay
CSC	Constant Serum Concentration (assay format)
CV	Coefficient of variation
DMEM	Dulbecco's Modified Eagle Medium
FBS	Fetal bovine serum
FLuc	Firefly luciferase
HEK293T	Human embryonic kidney 293T cell line
IgG	Immunoglobulin G
MCMC	Markov chain Monte Carlo
MOI	Multiplicity of infection
NAb	Neutralizing antibody
ND50	50% neutralizing dose (serum dilution giving 50% inhibition)
NLuc	NanoLuc luciferase
PBS	Phosphate-buffered saline
PCR	Polymerase chain reaction
PEI	Polyethylenimine
qPCR	Quantitative polymerase chain reaction
RLU	Relative light units
SV40	Simian virus 40
VSC	Variable Serum Concentration (assay format)
vg	Viral genome (vector genome)
WPRE	Woodchuck hepatitis virus post-transcriptional regulatory element

1 Introduction

Modern neuroscience increasingly depends on genetic tools to map, monitor, and manipulate defined neuronal populations *in vivo*. Viral vectors enable stable expression of reporters and actuators in targeted cells, supporting techniques such as activity imaging, optogenetics, chemogenetics, circuit tracing, and gene editing. Among available platforms, adeno-associated viruses (AAVs) are widely used, as they can be tailored for brain delivery, achieve sustained expression, and are compatible with diverse experimental approaches across a wide range of model species, from rodents to non-human primates.

While transgenic mouse lines have been instrumental in defining neuronal populations, they offer limited translational utility. In contrast, AAVs serve as a bridge between basic and clinical science: they are the vehicle of choice for delivering exogenes – from optogenetic actuators to CRISPR/Cas gene-editing systems – in both systems neuroscience and human therapy. This allows researchers to dissect neural circuits and validate therapeutic strategies using the exact same delivery platform intended for clinical use.

In clinical contexts, the same properties that make AAV valuable for research have already translated into therapeutic benefit, most notably for spinal muscular atrophy and inherited retinal dystrophies. Parallel developments extend beyond the nervous system to conditions such as hemophilia. Several AAV-based therapies have already gained regulatory approval, and many more are in active clinical development across neurology, ophthalmology, and systemic indications (1–4).

However, a major obstacle to the broader application of AAV-based therapies is the presence of neutralizing antibodies (NAbs) targeting the viral capsid. These antibodies compromise both safety and efficacy, presenting significant challenges for patients with pre-existing immunity, those requiring repeat dosing, or individuals with heightened immune sensitivity (5–8).

NAbs typically arise following natural infection with wild-type AAVs or through cross-reactive immune responses triggered by other parvoviruses (9–12). Additionally, patients previously treated with AAV-based gene therapy can develop robust anti-AAV immunity, leading to rapid vector clearance upon re-administration (13,14).

Mechanistically, NAbs inhibit vector binding to target cell receptors, promote immune-mediated opsonization, and activate complement pathways. Collectively, these processes reduce or abrogate transduction and therapeutic efficacy (15,16). Even low NAb levels can impair efficacy, underscoring the need for sensitive and reliable detection to support patient eligibility, dose selection, and long-term treatment strategies.

Pre-existing immunity to AAV is widespread across populations and varies by serotype and geography (6,17,18). Serological surveys at a 1:1 serum dilution report NAbs against AAV1, AAV5, and AAV9 in 74.9%, 63.9%, and 57.8% of adults, respectively (5). These prevalence data define eligibility thresholds and dosing/re-dosing strategies, while driving capsid-engineering efforts to develop AAV variants with improved immune evasion.

Animal models used for translational neuroscience exhibit similar or analogous immunity to AAVs. Large animals frequently harbor neutralizing antibodies that can hamper vector performance. Consequently, screening animals for pre-existing immunity is necessary to avoid misinterpreting neutralization-mediated failure as lack of vector potency or biological variability (7,9,19).

Various approaches have been explored to overcome the impact of pre-existing neutralizing antibodies, including transient immunosuppression, capsid engineering for epitope masking, exosome-enveloped AAV for immune evasion, and plasmapheresis to deplete circulating IgG before therapy (20–30). However, regardless of the mitigation strategy employed, therapeutic success depends on the ability to accurately quantify NAb levels before and after intervention. Therefore, reliable neutralization assays remain a foundation for clinical decision-making.

NAbs are typically measured using functional assays that quantify the ability of blood serum to inhibit AAV transduction *in vitro*. For clinical application, these methods need to be robust, well-documented, and standardized so that measured inhibition correlates reliably with therapeutic outcomes. Currently, however, assays are developed independently by individual laboratories and companies, leading to differences in design, sensitivity, threshold definitions, and data interpretation. Consequently, cross-study comparison, regulatory evaluation, and clinical decision-making are difficult. Recent studies (31–34) have reported these discrepancies across neutralization assays, including

divergent cutoffs, detection limits, and cell-based formats, which in turn can contribute to inconsistent trial outcomes.

This lack of harmonization, together with technical artifacts that obscure partial neutralization, highlights the need for a unified method that combines an optimized experimental design with a rigorous analytical strategy. In response, I developed the core Transduction Inhibition Assay (coreTIA), a framework that integrates an optimized constant serum concentration assay format with a Bayesian statistical analysis pipeline. The constant serum concentration design stabilizes baseline transduction and reduces matrix effects that confound conventional dilution protocols, thereby improving sensitivity and revealing partial neutralization that might otherwise be missed. In parallel, the Bayesian framework assigns credible intervals to each measurement estimate and remains accurate even when dilution series are incomplete, a frequent limitation when working with limited patient samples or unknown neutralization levels.

This combined experimental and statistical strategy was validated across multiple serotypes, including AAV1, AAV5, and AAV9. It enabled the reclassification of sera previously considered non-neutralizing and extended the detectable persistence of NAbs in preclinical seroreversion models involving both feline and rhesus macaque samples. By strengthening both the laboratory procedure and the statistical treatment, coreTIA offers a harmonized basis for NAb quantification that improves comparability across studies and enhances the reliability of patient stratification and trial outcomes.

2 Objectives

The primary aim of my thesis was to establish a harmonized method for quantifying AAV neutralizing antibodies that integrates experimental optimization with robust data analysis. By resolving current measurement discrepancies, the work sought to enhance patient stratification for gene therapy and facilitate the reliable translation of safety and efficacy data from essential preclinical models to clinical application.

1. **Identification of key assay parameters and establishment of an optimized protocol.**

   The first objective was to systematically assess existing assay variables to identify which factors most significantly impact assay performance and reproducibility. Based on this evaluation, the aim was to select optimal conditions and combine them into a core Transduction Inhibition Assay designed to increase robustness and sensitivity.

2. **Implementation of a statistical framework for quantifying neutralizing activity.**

   The second objective was to evaluate the limitations of conventional data analysis methods. The goal was to develop and implement a statistical workflow that provides reliable neutralization activity estimates and credible intervals.

3. **Comparative validation of the optimized core assay across human and animal models.**

   The third objective was to compare the performance of the newly developed core assay against standard methodologies. The aim was to determine whether the optimized design offers superior sensitivity for stratifying patient samples compared to conventional protocols. Furthermore, the objective included validating the assay's cross-species utility by characterizing immune responses in relevant preclinical models, ensuring it can support translational research.

3 Methods

3.1 Experimental Procedures

3.1.1 Bioluminescent assay reporters

To evaluate reporter sensitivity, I utilized plasmids encoding *CAG-FLuciferase-WPRE-SV40* and *CAG-NLuc-3xFLAG-10His-WPRE-SV40*. The *pAAV-CAG-NLuc-3xFLAG-10His-WPRE-SV40* plasmid was cloned by inserting the NLuc-3xFLAG-10His transgene from *pGWB701NL3F10H* (Addgene: 141288) into the tdTomato site of *pENN-AAV-CAG-tdTomato-WPRE-SV40* (Addgene: 105554) using BamHI and EcoRI restriction sites. The NLuc insert was amplified using the following primers:

Forward: 5' - GTGGATCCGCCACCATGGTCTTCACACTCGAAG

Reverse: 5'- GATGAATTCGAGCTCTCAGTGATGGTG

The *pAAV-CAG-FLuciferase-WPRE-SV40* plasmid was constructed by replacing tdTomato with Firefly luciferase from *pBV-Luc* (Addgene: 16539) using the same backbone. The luciferase transgene was PCR-amplified with the following primers:

Forward: 5' - GTGGATCCGCCACCATGGAAGACGCC

Reverse: 5' – GATGAATTCCATCACCATCACCATCACCACGGCGATCTTTCCGCCCTTC

These plasmids were subsequently used in AAV production to generate reporter vectors for neutralization assays.

3.1.2 AAV production

For AAV production, 80-100% confluent plates of HEK293T cells (ATCC, CRL-3216, Manassas, VA, USA) were cultured in DMEM supplemented with 10% FBS and 1% penicillin-streptomycin. The cells were cotransfected using polyethylenimine (PEI) and the following plasmids: pAAV vector plasmid containing the gene of interest, pHelper plasmid to provide adenoviral helper functions, and pRC plasmid containing rep and cap genes (DNA:PEI ratio of 1:4). 72 hours post-transfection, the cells were collected and lysed by repeated freeze-thaw cycles to release the viral particles. The AAV particles were purified using an iodixanol gradient ultracentrifugation method. The supernatant was layered onto a pre-made iodixanol gradient and centrifuged at 50,000 × g for 90 minutes at 16°C. The AAV-containing fraction was carefully extracted from the gradient.

The extracted fraction was then concentrated and buffer exchanged into PBS using an Amicon Ultra-15 centrifugal filter unit.

The viral genome (vg) titer was determined using quantitative PCR (qPCR). While the empty-to-full capsid ratio was not determined, potential variability from this parameter was controlled by ensuring that each direct comparison between assay methods utilized the same viral batch. The AAV preparation was aliquoted and stored at -80°C until use.

3.1.3 Variable Serum Concentration (VSC) Assay

Based on published protocols (9,35,36,18,37–40), I implemented the Variable Serum Concentration assay as follows: HEK293T cells were maintained in DMEM supplemented with 10% FBS and 1% Penicillin/Streptomycin. On the day of transduction, the *Cell Plate* was prepared by seeding 1×10^5 cells in DMEM supplemented with 1.25% FBS (total volume: 80 µL) into poly-L-lysine-coated black-wall, clear-bottom 96-well plates. The plate was then incubated at 37 °C with 5% CO_2 for 2 hours (Figure 1).

To prepare the *Transduction Mix*, a two-fold serial dilution of blood serum was prepared in DMEM. The *AAV Mix* was prepared in DMEM at a constant viral input of 1×10^7 vg per well (MOI 100). The *AAV Mix* was then combined with the diluted serum in equal volumes, resulting in an additional two-fold dilution. The *Transduction Mix* was incubated at 37 °C for 1 hour, after which 20 µL was added to each well of the *Cell Plate*. DMEM was used as the *Antibody-free Control*. The plate was incubated at 37 °C with 5% CO_2 for 24–48 hours. Exact amounts of components used for a VSC assay run are detailed in Table S1.

For luminescence measurement, half of the medium was removed from each well and replaced with Nano-Glo assay reagent (Promega, N1130, Madison, WI, USA), prepared according to the manufacturer's instructions. Luminescence was measured using a Cytation 5 multimode reader (BioTek Instruments, Winooski, VT, USA).

3.1.4 coreTIA: The Constant Serum Concentration (CSC) Assay

Unlike the Variable Serum Concentration assay, where the total serum concentration varies across dilutions, this method maintains a constant total serum concentration by diluting the test serum in FBS. HEK293T cells were seeded in DMEM without FBS into

poly-L-lysine-coated black-wall, clear-bottom 96-well plates. The *Transduction Mix* was prepared by diluting blood serum in FBS, and FBS served as an *Antibody-free Control* (Figure 1). Exact amounts of components used for a CSC assay run are detailed in Table S1. All other steps were identical to the Variable Serum Concentration assay.

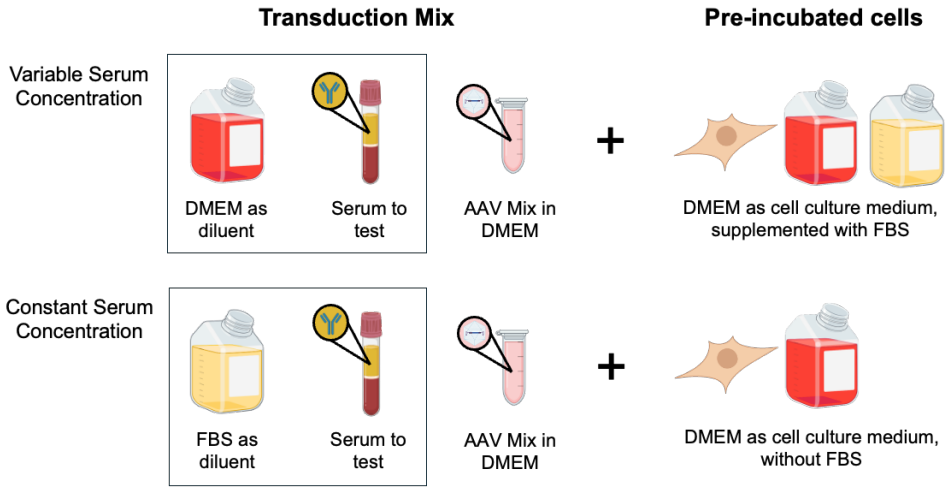

Figure 1. Schematic comparison of Variable Serum Concentration (VSC) and Constant Serum Concentration (CSC) assays. *The top panel depicts the Variable Serum Concentration approach, where DMEM serves as the diluent for test serum, resulting in varying total serum concentrations across dilutions. Pre-incubated HEK293T cells are maintained in DMEM supplemented with FBS. The bottom panel shows the Constant Serum Concentration approach, where test serum is diluted in FBS rather than DMEM, maintaining consistent total serum concentration across all dilutions. For this method, cells are cultured in DMEM without FBS supplementation. Both assays involve preparing a transduction mix containing the test serum and AAV vectors, that is pre-incubated before addition to cells, followed by measurement of transgene expression. Created with BioRender.com*

3.1.5 Assay calibration with monoclonal antibody

To calibrate the neutralization assay, a monoclonal anti-AAV9 antibody (ADK9) (Progen, Cat. #690162, Heidelberg, Germany) was tested against AAV9. Serial dilutions of the antibody were prepared to generate a calibration curve. The tested concentration range per well was 3.125–0.05 ng/mL. For VSC, the monoclonal antibody was first diluted in DMEM to achieve the desired concentration and total volume. Subsequently, a

twofold serial dilution series was performed in DMEM. For CSC, the monoclonal antibody was initially diluted in FBS. The twofold dilution series was then carried out using FBS as the diluent.

3.1.6 Systematic evaluation of serum content during pre-incubation

To generate data for the "Serum on cells" condition (Figure 3E and Figure S1), HEK293T cells were seeded in DMEM supplemented with increasing concentrations of FBS (0%, 1.25%, 6.25%, and 12.5%), while the AAV mix was prepared in DMEM without FBS. The cells were incubated for 2 hours at 37°C, and the AAV mix was incubated separately for 1 hour at 37°C before being added to the wells.

For the "Serum on AAV" condition, instead of incubating the cells with FBS, the AAV mix was pre-incubated with varying concentrations of FBS (0%, 5%, 25%, and 50%) for 1 hour at 37°C before being added to the cells.

In both conditions, 80 µL of cell suspension was seeded into each well, followed by the addition of 20 µL of AAV mix, resulting in a final volume of 100 µL per well. The final FBS concentration after mixing with the cells was 0%, 1%, 5%, and 10%. Luminescence was measured 24 hours post-transduction.

In the experiment using seronegative human serum, all experimental steps remained identical, except that human serum was used in place of FBS. Transduction efficiency was calculated by normalizing the RLU values to the 0% serum condition.

3.1.7 Acquisition of serum samples

Blood samples were collected from subjects following standard procedures. Whole blood was collected in red-top blood collection tubes, serum separator tubes, or sterile Eppendorf tubes and allowed to clot at room temperature for 30 minutes. Samples were then centrifuged at 2,000 × g for 10 minutes at 4°C to separate the serum. The supernatant (serum) was carefully aspirated to avoid disturbing the clot and transferred into sterile tubes. Serum was aliquoted into single-use volumes to prevent repeated freeze-thaw cycles, ensuring sample integrity. Aliquots were stored at -80°C until use. Required aliquots were thawed on ice and mixed gently to ensure homogeneity.

Samples from 46 human donors were used in this study, collected at Semmelweis University, Faculty of Medicine, Department of Ophthalmology, approved by the Institutional Scientific Research Ethics Committee of Semmelweis University. All human

participants provided written informed consent before participation. Animal experiments followed the guidelines set by the Directive 2010/63/EU. Mouse experiments were approved by the Animal Care Committee of the Research Centre for Natural Sciences of the Hungarian Academy of Sciences and the National Food Chain Safety Office of Hungary. Adult C57/Bl6 mice were parenchymally injected with AAV9 encoding a fluorescent protein under the control of hsyn promoter (10^9 vp delivered). After one week, blood was collected via cardiac puncture after euthanasia. Serum samples from six (domestic short hair, mixed sex, 1–4 years old) cats were included in the study. Four subjects had no AAV injections prior to sampling (Figure 3). One subject (Figure 4A-B) was vaccinated with the feline CRP vaccine, which provides protection against Calicivirus, Rhinotracheitis virus, and Panleucopenia virus. Feline panleukopenia virus, a type of parvovirus, is known to cross-react with AAV (9). Another subject (Figure 4C-F) was injected with CAP-B22 (41). All procedures were approved by the Animal Care Committee of the HUN-REN Research Centre for Natural Sciences and by the National Food Chain Safety Office of Hungary. Macaques (Macaca mulatta, mixed sex, age between 9-21 years old) received no AAV injections before sampling, their care and experimental procedures complied with the National Institute of Health's Guide for the Care and Use of Laboratory Animals, the European legislation (Directive 2010/63/EU) and were approved by the Ethical Committee of KU Leuven or with the Animal Welfare Committee of the University of Pécs, permission issued by the Department of Animal Health and Food Control of the County Government Offices of the Ministry of Agriculture.

3.1.8 Heat-inactivation

To evaluate the effect of heat inactivation, blood serum and FBS were incubated at 56°C for 30 minutes before use in the assay.

3.2 Statistical and Computational Framework

3.2.1 ND50 definition

In this work, I define ND50 (Neutralizing Dose for 50% inhibition) as the dose – expressed as a serum dilution or an antibody concentration – required to reduce transduction by 50% relative to the *Antibody-free Control*.

3.2.2 Synthetic data generation

In cell-based assays, variability arises from multiple sources, including biological, technical, and instrumental factors. Biological variability – such as differences in cell viability, transduction efficiency, and intracellular enzyme activity – tends to scale with signal intensity, making log-normal (multiplicative) noise a suitable model (42). This model aligns with empirical observations from luminescence-based assays, where variability increases proportionally with signal intensity, rather than remaining constant. Synthetic datasets generated using this noise model were used to evaluate the performance of different ND50 estimation methods under controlled conditions.

3.2.3 Non-statistical 50% inhibition estimation

ND50 is defined as the first dilution at which the mean response is <50% of the *Antibody-free Control*. While this approach offers simplicity and has been widely adopted in the field, it does not provide measure of uncertainty for the ND50 estimate.

3.2.4 Linear-bootstrap 50% inhibition estimation

The Linear-bootstrap method focuses on the region of the dose-response curve where the measured transduction crosses the 50% threshold. Specifically, it identifies the two adjacent data points that bracket 50% transduction (one above and one below 50%) and uses all possible combinations of technical replicates at those two points to perform a simple linear interpolation. For each combination, the method solves for the x-value (dose or dilution) at y=50%, generating a distribution of ND50 values. The mean of these bootstrapped ND50 estimates provides a point estimate, while the spread of values naturally yields a credible interval (e.g., 2.5th–97.5th percentiles). This computationally simple method avoids fitting an entire dose-response curve while providing statistical estimates of uncertainty but requires data points that bracket the 50% neutralization threshold to perform interpolation.

3.2.5 Hill-MCMC 50% inhibition estimation

I implemented a Bayesian Markov Chain Monte Carlo (MCMC) approach to fit a Hill curve to dose-response data. Measurement noise was accounted for using either empirical standard deviations computed from replicate measurements, or a fixed noise assumption when only single replicates are available ($\sigma = 0.05$, based on typical assay variability).

The probabilistic model included truncated normal priors for the slope ($\mu = 1$, $\sigma = 0.05$) and ND50 (μ = mean (tested dilution range), $\sigma = 0.15$), and a half-normal prior ($\sigma = 0.5$) for the lower bound of the Hill curve. Log-transformed observed data were modeled using a normal likelihood centered on the Hill function predictions. Posterior distributions were sampled (n=2000 draws, 800 tuning steps, 0.95 target acceptance, $R<1.01$ convergence threshold) via MCMC to infer their credible intervals for Hill parameters under uncertainty or limited replicate conditions.

3.2.6 Two-Stage Interval Estimation Approach for ND50 Uncertainty (CI-of-CIs)

I implemented a two-stage interval estimation approach to characterize the distribution of uncertainty in ND50 estimation across different experimental designs. In the first stage, each sampling of the noise-contaminated data yields a Bayesian credible interval (2.5th–97.5th percentiles) for ND50. In the second stage, I aggregate those credible intervals across all simulations to produce a single, composite uncertainty interval (confidence interval of credible intervals, CI-of-CIs).

Rather than simply averaging intervals - which can underestimate variability - this meta-analysis of credible intervals integrates both experimental noise and model-fitting uncertainty, yielding a more conservative and robust measure of true uncertainty, especially when technical replicates vary or the true ND50 lies outside the tested dilution range.

3.2.7 Bayesian Threshold Test for Practical Equivalence of ND50 Estimates

To distinguish meaningful differences in ND50 from technical variability, I implemented a Bayesian threshold test based on the absolute log2-difference between group means exceeding a data-driven practical variability threshold. This approach models the log2-transformed ND50 observations within each group as normally distributed around their respective group mean (μ_1, μ_2) and standard deviation (σ_1, σ_2) using a Bayesian hierarchical framework. Priors were assigned to these parameters: normal distributions centered on the sample mean of the log2-transformed data with a standard deviation of 0.5 were used for the group means (μ_1, μ_2), and half-normal distributions with a standard deviation of 0.5 were used for the group standard deviations (σ_1, σ_2). The posterior distribution for the difference between the group means, $\Delta = \mu_1 - \mu_2$, was derived using Markov Chain Monte Carlo sampling (2000 draws, 400 tuning steps, 0.95 target

acceptance, R<1.01 convergence threshold). From the posterior samples of Δ, I calculated the probability P(|Δ| > θ) as the proportion of samples where the absolute difference exceeded a given threshold θ. I defined two tests based on this probability: the Bayesian Difference Test uses θ = 0 to assess any non-zero difference (P_0 = P(|Δ|>0)), and the Bayesian Practical Equivalence Test uses θ = 0.3 log2 units to assess differences exceeding the practical threshold ($P_{0.3}$ = P(|Δ|>0.3)). I defined statistical significance if P_0 > 0.95 and practical significance (i.e., difference exceeding the technical threshold) if $P_{0.3}$ > 0.95. The 0.3 log2 threshold was chosen based on the 90th percentile of observed 95% Hill-MCMC credible interval widths across diverse samples and reflecting the typical intra-assay technical precision achieved with this method.

3.2.8 Data Analysis

The coreTIA data representation and documentation is built upon the Wellmap Python package (43), which serves as the foundation for handling well-based assay data such as those from neutralizing antibody assays. Implementing this formalized pipeline enhances experimental documentation, traceability, and reproducibility.

To assess the effect of applying serum in different conditions (Figure 3 and Figure S1) or the effect size between VSC and CSC, I compared transduction values normalized to either 0% FBS (Figure 3 and Figure S1) or to the *Antibody-free Control*. To quantify effect size without assuming normality, I calculated Cliff's delta, a non-parametric measure suitable for small sample sizes. Cliff's delta measures the degree of overlap between two distributions and ranges from -1 to +1, where 0 indicates complete overlap (no effect), and absolute values of 0.11, 0.28, and 0.43 represent small, medium, and large effects, respectively (44). For each comparison, I computed Cliff's delta as abs(greater - lesser)/total, where "greater" counts the number of times a value from the first group exceeds a value from the second group, "lesser" counts the reverse, and "total" is the product of the two sample sizes. This approach provides a robust estimate of effect size that complements the permutation test p-values.

To estimate ND50 values, raw luminescence data were first converted to a percentage of inhibition relative to the serotype-matched, *Antibody-free Control*. This ratiometric analysis mathematically normalizes for baseline differences in transduction efficiency between serotypes, ensuring the resulting dose-response data provide a valid and comparable measure of functional neutralizing activity.

To derive ND50 estimates from these normalized data, I employed modeling strategies detailed above, tailoring the approach to the specific data quality produced by each assay format. For the ADK9 monoclonal antibody experiments, which consistently yielded complete sigmoidal dose-response data in both VSC and CSC formats, I used a four-parameter Hill curve fitted via a Bayesian Markov Chain Monte Carlo method. In contrast, VSC assays using complex biological sera often produced incomplete or non-sigmoidal data, making a Hill curve fit unreliable. Although the CSC format consistently restored a well-behaved sigmoidal shape to these serum samples, a more robust linear model was necessary for direct comparison. Therefore, to ensure a fair and direct analytical comparison between the VSC and CSC methods, I consistently applied this linear model to all datasets involving serum samples.

4 Results

4.1 Identification of critical assay parameters and establishment of an optimized protocol.

4.1.1 A major obstacle: Inflated transduction baselines and matrix effects in conventional AAV NAb assays

Conventional cell-based adeno-associated virus (AAV) neutralization assays, widely used in both research and clinical screening, typically employ a variable serum concentration (VSC) protocol in which test sera are serially diluted in cell culture medium (9,18,35–40). To validate this assay format, I first tested the monoclonal anti-AAV9 antibody (ADK9) against AAV9, which produced a sigmoidal dose-response curve where transduction increased as the antibody concentration decreased by serial dilution. This inhibitory response allowed for estimation of the Neutralizing Dose 50 (ND50), defined as the serum dilution at which 50% inhibition of transduction is observed (Figure 2A). This result confirms the assay's capability to measure neutralizing activity under controlled conditions.

However, when applied to complex biological samples, specifically human sera, a different phenomenon emerged. Instead of the typical sigmoidal curve, most human serum samples unexpectedly showed increasing transduction levels as the serum concentration increased from 1/128 to 1/4 dilution (Figure 2B). This behavior deviates markedly from the expected neutralization curve and from the flat profiles expected in seronegative individuals. The elevated transduction baseline suggests the presence of assay matrix effects that enhance rather than inhibit AAV transduction, masking true neutralization activity.

This matrix effect is not limited to the AAV9 serotype. Similar transduction enhancement at higher serum concentrations was observed for other AAV serotypes (AAV1 and AAV5) (Figure 2C-D), demonstrating that this is a more general phenomenon rather than a serotype-specific artifact.

A closer examination of these curves reveals further complexity. In many cases, transduction exceeds the nominal 100% set by the *Antibody-free Control*, compromising the reliability of the standard reference and making it difficult to interpret results. Some

donor samples showed a continuous increase in transduction efficiency across all dilutions, while others peaked and then declined gradually as serum concentration rises. Although this decline might hint at weak or partial neutralizing activity, transduction almost always remains above the 50% threshold required for ND50 calculation, leaving the potency of antibody-mediated inhibition unresolved. This methodological limitation needs to be addressed to ensure reliable eligibility testing.

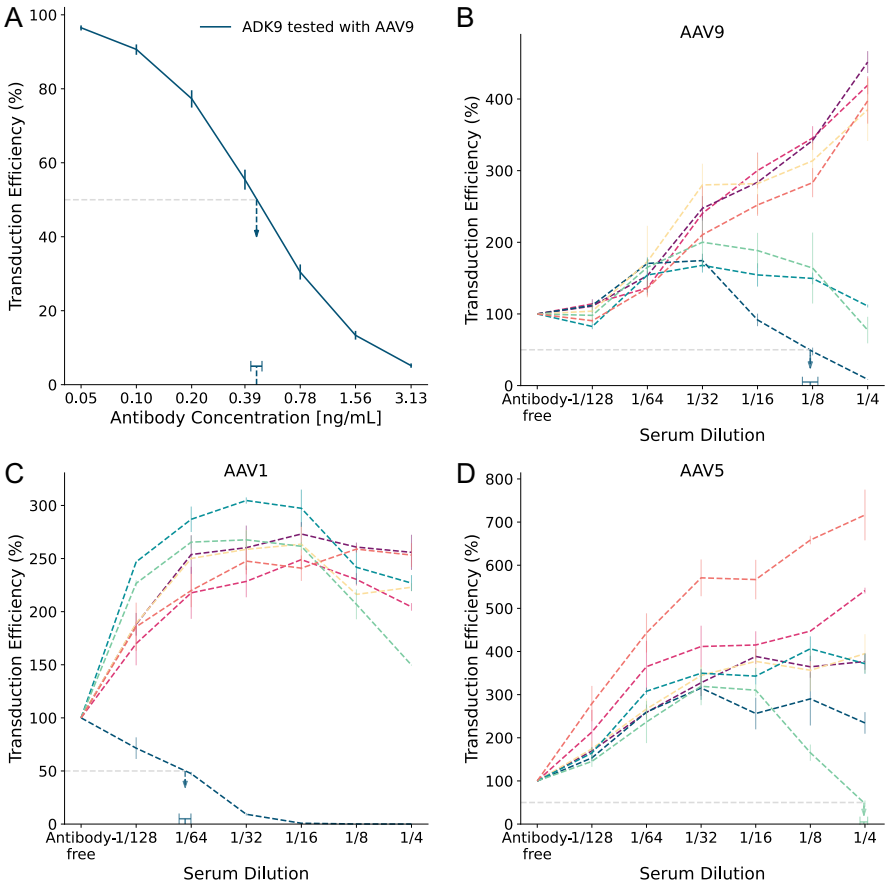

Figure 2. Limitations of the conventional Variable Serum Concentration (VSC) assay. ***(A)*** *Neutralization curve for an anti-AAV9 antibody (ADK9) tested against AAV9 using the VSC format, showing expected sigmoidal inhibition. Vertical error bars denote 95% credible intervals, and the vertical dashed arrow pointing to the horizontal bar indicates the ND50 estimate and its uncertainty range (Methods).* ***(B-D)*** *Transduction curves for seven human sera tested against AAV9, AAV1, and AAV5 using the same VSC assay. Each color represents a different donor, same color denotes same donor across panels; the x-axis shows 2-fold serum dilutions, and the y-axis shows transduction efficiency relative to an antibody-free control.*

Taken together, these atypical curve shapes suggest that, in many human samples, the readout is strongly influenced by factors other than antibody-mediated neutralization, limiting the usefulness of the conventional VSC assay format for eligibility assessment. Given that the main procedural difference between these experiments and the initial ADK9 validation was replacing a purified monoclonal antibody with human serum, I hypothesized that the increasing serum content itself might be responsible for the unexpected rise in transduction.

Serum is a complex matrix containing albumin, lipoproteins, complement and coagulation factors, cytokines and other proteins that can, in principle, influence multiple steps of the assay: viral attachment and entry, cell viability, and the cellular capacity to produce the reporter protein (15,45). Thus, changes in serum concentration may modulate the measured signal independently of AAV-specific neutralizing antibodies.

To test this hypothesis, I next examined how both the amount of serum and the way it is introduced into the assay influence transduction efficiency. I compared two configurations: a "Serum on cells" setting, where serum was present only in the cell culture medium, and a "Serum on AAV" setting, where serum was first mixed with the AAV before adding it to the cells (Figure 3A). As an antibody-free surrogate for human serum, I used fetal bovine serum (FBS).

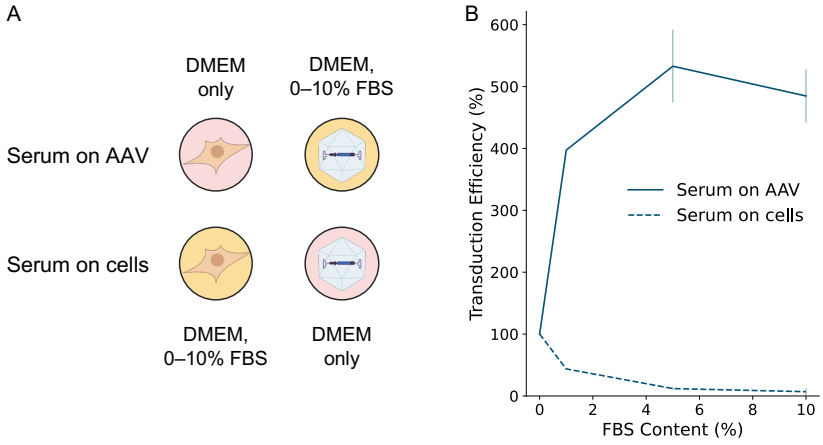

Figure 3. Serum pre-incubation strategy influences AAV transduction efficiency.

(A) *Schematic overview of two pre- incubation strategies under antibody-free serum conditions. Top: "Serum on AAV" denotes pre-incubation of AAV with different concentrations of FBS while cells are pre-incubated in DMEM only. Bottom: "Serum on cells" denotes pre-incubation of cells with different concentrations of FBS, while AAV is*

pre-incubated in DMEM only. ***(B)*** *Effect of FBS content during pre-incubation on transduction efficiency, normalized to the 0% FBS condition. Under "Serum on AAV", luminescence increases sharply and plateaus near 5% FBS, whereas under "Serum on cells," luminescence decreases as FBS content increases. Vertical error bars indicate standard deviations from the mean.*

In the "Serum on cells" condition, increasing FBS concentrations progressively reduced AAV transduction (Figure 3, dashed line), consistent with previous reports that high serum levels can inhibit vector entry or cell viability (46). In contrast, in the "Serum on AAV" condition, transduction showed a dose-dependent increase with increasing FBS concentration (Figure 3, solid line), indicating that pre-incubation of AAV with FBS promotes rather than suppresses transduction. This is in line with earlier studies showing that albumin and other serum components can enhance AAV transduction by associating with the capsid surface (46,47). At a final FBS concentration of 10%, the difference between these two modes of application was pronounced: transduction was substantially higher when FBS was pre-incubated with the vector than when the same amount of FBS was present only in the cell culture medium.

This dual role of FBS – acting as an inhibitor when present only on cells, but as an enhancer when pre-incubated with AAV – was consistently observed across multiple capsid types (Cliff's delta ≈ 1.0 for all conditions above 0% serum; Methods, Figure S1A–D), indicating that serum components can modulate AAV transduction through distinct mechanisms depending on whether they act primarily on the cells or on the viral particles. FBS provides a convenient antibody-free matrix for assay calibration due to its availability, but its non-human origin means it may not fully represent the properties of human serum. To assess whether the observed matrix effects extend to human samples, I repeated the "Serum on cells" and "Serum on AAV" experiments using seronegative human serum instead of FBS. The results closely mirrored the FBS data: higher concentrations of human serum reduced transduction in the "Serum on cells" condition, but enhanced transduction when pre-incubated with AAV in the "Serum on AAV" condition (Figure S1E-H). This parallel effect indicates that the dual role of the serum matrix is not specific to FBS and supports the use of FBS as a practical surrogate for seronegative human serum during assay calibration.

4.1.2 Stabilizing baseline transduction with constant serum concentration

The limitations of the conventional variable serum concentration (VSC) assay for AAV neutralizing antibody detection highlighted the need for a method that could minimize matrix-induced enhancement and provide a stable baseline for quantification.

To address this, I developed and validated the core Transduction Inhibition Assay (coreTIA), a constant serum concentration (CSC)–based protocol. Unlike the VSC format, where serum is diluted in cell culture medium, the coreTIA framework maintains total serum content constant across all assay dilutions by mixing the test sample with FBS, an antibody-free diluent. This design stabilizes transduction baselines and minimizes confounding enhancement, enabling sensitive and quantitative measurement of neutralizing activity.

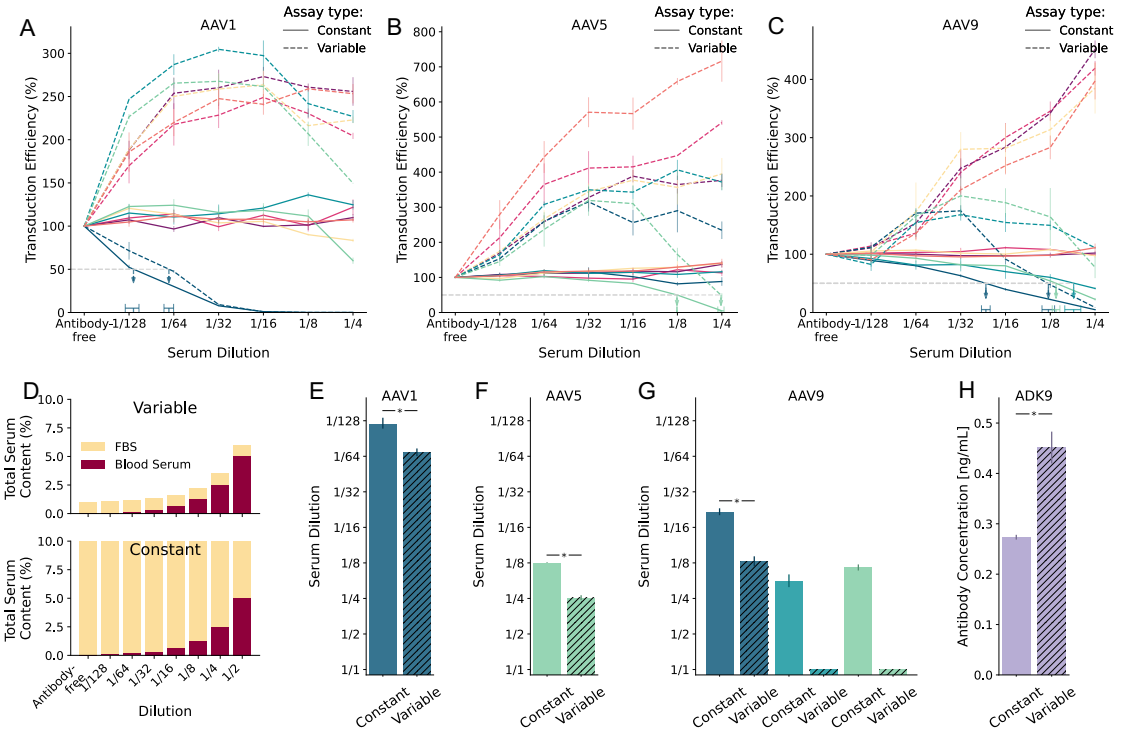

Figure 4. Optimized pre-incubation conditions and constant serum concentration yield an improved AAV neutralization assay across different serotypes.

(A-C) *Transduction curves for seven human sera tested against AAV9, AAV1, and AAV5. Each color represents a different donor, same color denotes same donor across panels; the x-axis shows 2-fold serum dilutions, and the y-axis shows transduction efficiency relative to an antibody-free control. Solid lines (Constant) stay near 100% for non-*

neutralizing samples, whereas dashed lines (Variable) can exceed 100% due to changing total serum. The blue, teal, and green curves report neutralizing activity sufficient to reach the ND50 within the tested dilution range. ND50 dilutions for neutralizing samples are marked by vertical dashed arrows pointing to horizontal bars indicating 95% credible intervals (Methods). Throughout panels, Constant refers to the CSC method where total serum remains fixed at 10%, while Variable refers to the VSC method where total serum concentration increases with less dilution. ***(D)*** *Schematic illustration of design differences between Variable Serum Concentration (VSC, Variable in legends) versus Constant Serum Concentration (CSC, Constant in legends) assay formats. In VSC, total serum changes with each dilution step because test serum is added on top of a fixed FBS level; in CSC, total serum is held at 10% throughout, differing only in the proportion of test serum to FBS.* ***(E-G)*** *Bar plots comparing neutralization values (ND50) for the neutralizing sera against AAV9, AAV1, and AAV5 (as shown on B-D). Constant (filled bars) yields significantly higher values than Variable (striped bars). Asterisks denote significant difference (Methods). For samples exhibiting minimal (ND50 < 1/4) or no neutralization, 1/1 dilution is used as placeholder.* ***(H)*** *Sensitivity comparison of Constant vs. Variable using a dilution series of ADK9 against AAV9. Constant shows significantly greater sensitivity.*

When the same donor samples were retested using the CSC-based coreTIA format, transduction curves for truly non-neutralizing donors showed transduction efficiencies consistently close to 100% across all capsids, reflecting the expected profiles in the absence of neutralizing antibodies (Figure 4A-C). Importantly, several samples previously classified as non-neutralizing by the VSC format (where transduction remained elevated above 50%) revealed clear neutralization under the CSC conditions, with transduction dropping below the 50% threshold. This result uncovered neutralizing antibodies that were masked by matrix effects in the variable format. For samples with neutralizing antibodies, ND50 values measured by coreTIA were significantly higher than those derived from the VSC assays (Bayesian Practical Equivalence Test, Methods section), indicating improved sensitivity.

A dilution series of the ADK9 monoclonal antibody used as an internal benchmark further supported this conclusion: compared to the VSC, the CSC format detected neutralization

at lower antibody concentrations (Figure 4H, Figure S2), confirming its improved performance for NAb quantification.

4.1.3 Implementation of the High-Sensitivity NanoLuc Reporter System

The successful elimination of matrix effects via the CSC format provided a stable baseline, yet the assay's sensitivity depends on the reporter system employed. While Firefly luciferase (FLuc) remains a standard tool in the field, its limited dynamic range can obscure low-level neutralizing activity. To overcome this, I integrated the NanoLuc (NLuc) luciferase reporter, known for its superior brightness and stability (48–50), into the coreTIA framework.

Direct head-to-head comparison in HEK293T cells confirmed the substantial difference in performance between the two reporters. NLuc yielded signal intensities approximately 1000-fold higher than FLuc under identical conditions (Figure 5A-C). Specifically, at a multiplicity of infection (MOI) of 100, NLuc reliably generated luminescence in the range of ~10^5 relative light units (RLU) – well above the noise threshold – whereas FLuc signals remained near the limit of reliable quantification (~10^2 RLU). Beyond signal intensity, NLuc demonstrated strong linearity, maintaining a proportional signal response across AAV1, AAV5, and AAV9 over a broad viral load range (AAV1, AAV9: MOI 10–1,000; AAV5: MOI 10–10,000). This cross-serotype consistency is essential for a modular assay intended for broad clinical application.

Determining the optimal viral load required balancing analytical sensitivity with assay robustness. To identify this balance point, I evaluated neutralizing activity in human sera at MOIs of 10, 100, and 1000 (Figure 5D-E).

High viral input (MOI 1000) reduced sensitivity, due to the saturation of neutralizing capacity by excess viral particles. Conversely, minimizing viral load to MOI 10 theoretically maximizes sensitivity. However, the data showed that this benefit was inconsistent – significant only for AAV9, but negligible for AAV1 or AAV5 (Figure 5E). Furthermore, such low viral inputs introduce stochastic variation, where random fluctuations in viral entry compromise signal reproducibility.

Considering these factors, I selected MOI 100 for the coreTIA protocol as it provides a practical balance, delivering high sensitivity that performs consistently across multiple serotypes. This choice prioritizes the development of a robust, broadly applicable assay over maximizing sensitivity for a single serotype.

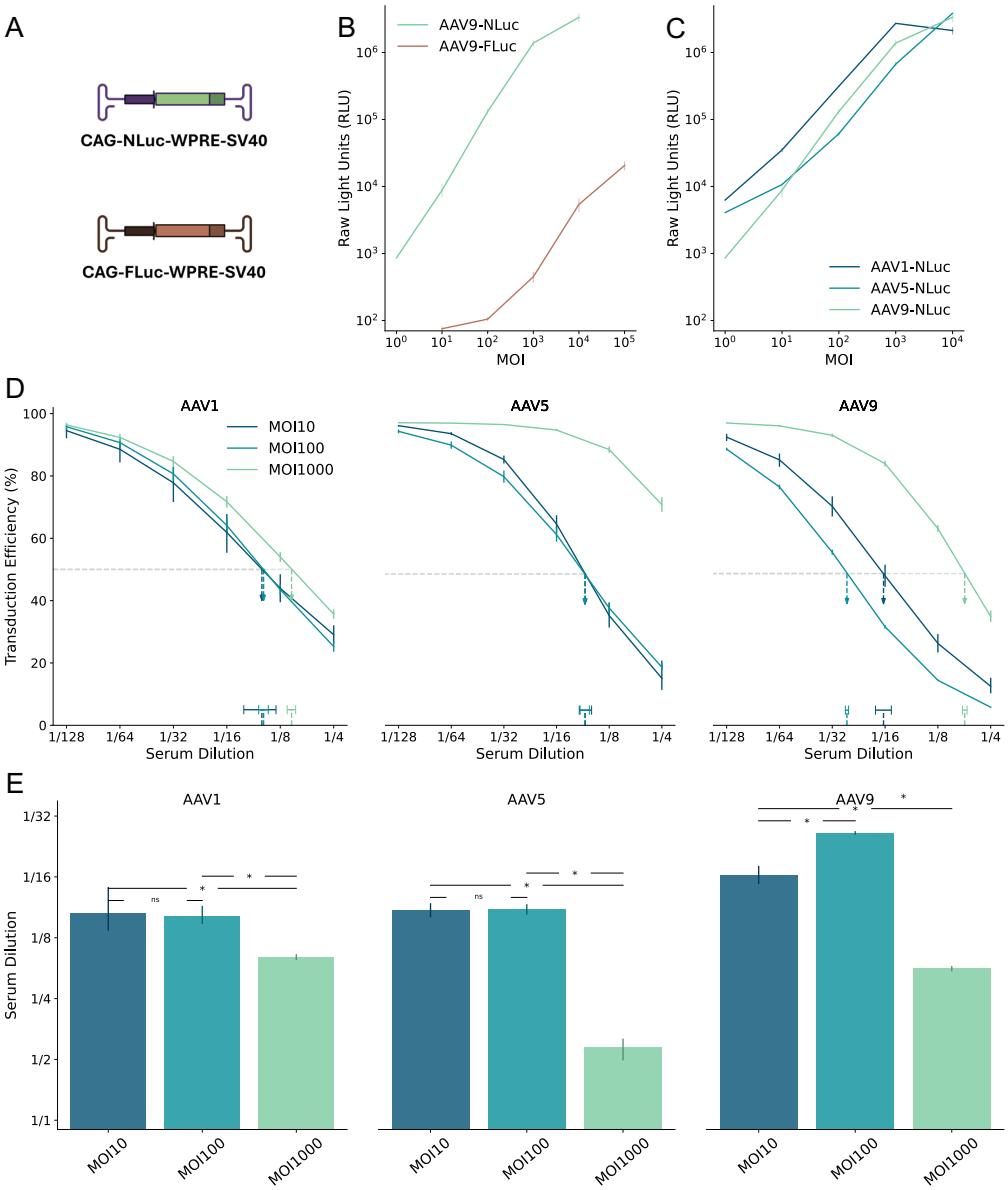

Figure 5. NanoLuc at MOI 100 provides high sensitivity across AAV capsids.

(A) *Schematic diagrams of plasmids encoding NanoLuc (NLuc) and Firefly luciferase (FLuc) reporters.* ***(B)*** *Dynamic range of AAV9-FLuc versus AAV9-NLuc transduction assays over a range of multiplicities of infection (MOIs). NLuc exhibits approximately three orders of magnitude higher signal intensity than FLuc at equivalent MOIs. Error bars represent standard deviation across replicates.* ***(C)*** *Broad utility of NLuc reporter assays demonstrated across AAV1, AAV5, and AAV9 capsids. NLuc consistently maintains robust signal output across varying MOIs, with serotype-specific patterns of signal increase on the logarithmic scale. Error bars represent standard deviation across replicates.* ***(D)*** *Neutralization curves from the coreTIA with human serum for AAV1,*

AAV5, and AAV9 capsids. Different colors represent MOI 10 (teal), MOI 100 (orange), and MOI 1000 (purple). Horizontal dashed line denotes 50% transduction efficiency level. Dashed vertical arrows pointing to horizontal bars indicate the ND50 estimates (serum dilution at 50% inhibition) using Hill-MCMC. Vertical error bars on the data points represent standard deviation of transduction efficiency measurements across replicates. The legend in the left sub-panel applies to all three sub-panels. ***(E)*** *Summary of ND50 values across AAV capsids and MOIs. Statistical significance was determined using Bayesian Practical Equivalence Test (Methods, ns = not significant, * = significant difference exceeding practical threshold). Error bars represent 95% credible intervals from Hill-MCMC model evaluations.* ***(D, E)*** *The y-axis label ("Serum Dilution") of the left panel applies to middle and right panels.*

4.1.4 Determining assay parameters that affect sensitivity

To further refine the coreTIA protocol, I evaluated specific assay parameters to explore potential gains in implementation simplicity without compromising sensitivity.

First, I assessed the necessity of serum heat-inactivation, a common practice intended to minimize complement interference (32). Contrary to expectations, heat-inactivation (56°C, 30 min) of a neutralizing human serum sample significantly reduced the measured ND50 from ~1/8 to ~1/4, indicating lower detected neutralizing activity (Figure 6A). This loss of sensitivity aligns with findings that complement activation has minimal impact in HEK293T-based AAV assays (35,51). Consequently, the coreTIA protocol omits heat-inactivation to preserve optimal analytical sensitivity.

Next, I investigated the impact of temporal variables. Varying the incubation time of the Transduction Mix (15, 30, and 60 minutes) yielded statistically equivalent ND50 levels (Figure 6B), indicating that antibody binding reaches equilibrium rapidly. This flexibility allows for efficient processing of multiple plates. Similarly, comparing post-transduction readout times revealed that a 24-hour incubation is sufficient; ND50 values were consistent with those obtained at 48 hours (Figure 6C), enabling a shorter experimental timeline while maintaining data quality.

To complement human serum data with a controlled system, I assessed how *in vivo* exposure to AAV9 influences neutralizing activity. Mice received local AAV9 injections into the primary visual cortex at increasing doses (10^7, 10^8, 10^9 and 10^{10} genome copies).

A clear dose-dependent response was observed (Figure 6D): the highest dose (10^{10} vg) elicited a strong neutralizing response (ND50 > 1/8192). The 10^9 vg dose also produced a high neutralizing response, with an ND50 between 1/4096 and 1/8192. In contrast, the 10^8 vg dose resulted in a markedly lower ND50 of approximately 1/20. The lowest dose (10^7) failed to trigger a detectable response. These results demonstrate the ability of coreTIA to capture a broad dynamic range of neutralizing activity under tightly controlled conditions.

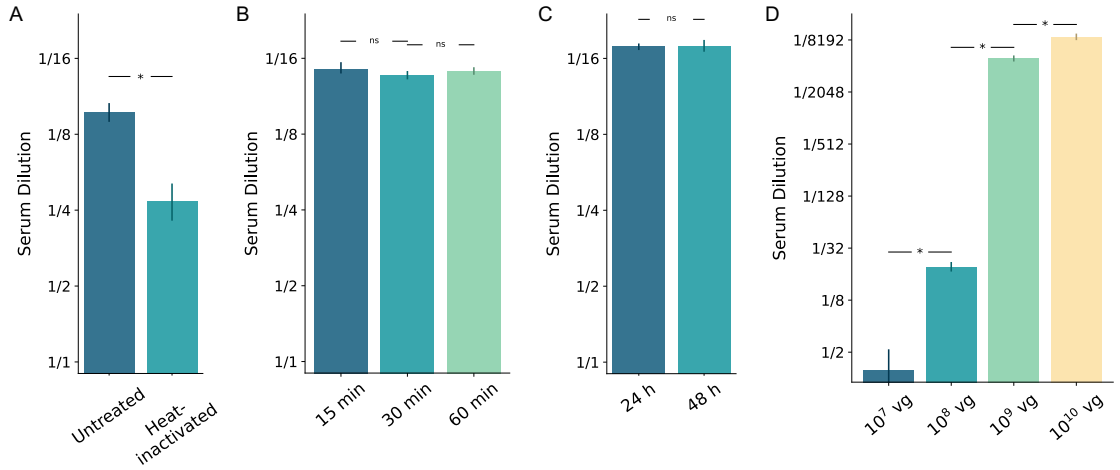

Figure 6. Optimization of coreTIA components.

Example assay runs underlining the relative importance of assay parameters. ***(A)*** *Heat inactivation: ND50 values for a human serum sample tested against AAV9-NLuc (MOI 100) under untreated vs. heat-inactivated (56°C for 30 minutes) conditions. Heat inactivation significantly reduces the measured ND50 (from ~1/8 to ~1/4), indicating lower detected neutralizing activity.* ***(B)*** *Transduction Mix incubation: ND50 values for a different human serum sample estimated after 15, 30, or 60 minutes of incubation at 37°C in a Transduction Mix containing the human serum, FBS, and AAV9-NLuc (MOI 100).* ***(C)*** *Post-transduction duration: ND50 values for the same serum sample as in panel B measured against AAV9-NLuc (MOI 100) at 24 and 48 hours post-transduction.* ***(D)*** *In vivo immunization: ND50 values determined one week after parenchymal administration of escalating doses of AAV9-GFP (1E+10, 1E+9, 1E+8, 1E+7 viral particles) in four individual mice, measured against AAV9, demonstrating dose-dependent induction of neutralizing antibody responses.*

In all panels, bars represent ND50 estimates calculated using the Hill-MCMC method, higher serum dilution values indicate greater neutralizing activity, reflecting higher

assay sensitivity. Error bars show 95% credible intervals from Hill-MCMC fits. Statistical significance was determined using Bayesian Practical Equivalence Test with the previously established practical equivalence threshold of θ = 0.3 log2 units: "" indicates a difference above this threshold, while "ns" indicates no significant difference (i.e., practical equivalence, Methods).*

4.2 Implementation of a statistical framework for quantifying neutralizing activity.

4.2.1 Statistical framework of coreTIA for robust ND50 estimation

Beyond stabilizing assay baselines, a key objective of my work was to obtain reliable and quantitative estimates of neutralizing activity. Conventionally, neutralizing antibody levels are determined by identifying the highest serum dilution that inhibits transduction by more than 50% relative to the *Antibody-free Control* (31). While straightforward and widely adopted, this threshold-based approach yields only a single point estimate, providing no information about measurement confidence or precision. This fundamental limitation becomes particularly acute when results fall near critical decision thresholds.

To address these constraints, I integrated the coreTIA framework with a Bayesian statistical pipeline that estimates neutralizing potency using two complementary methods: Linear-bootstrap estimation and Hill-MCMC modeling. Unlike the conventional method, both approaches generate credible intervals, explicitly quantifying the uncertainty of each measurement.

Using synthetic data with a known ground-truth ND50 of 1/16, both statistical methods produced estimates that were closer to the true value than the conventional non-statistical approach (Figure 7). With n = 50 samples, the mean ND50 converged to the same value while comparison of credible intervals revealed Hill-MCMC's advantage in precision. Paired t-tests for ND50 means showed no significant difference between the Linear-bootstrap and Hill-MCMC methods (Figure 7B, n = 50, t = 0.36, p = 0.72), whereas comparisons of Hill-MCMC vs Non-statistical (n = 50, t = 33.95, $p < 0.0001$) and Linear-bootstrap vs Non-statistical (n = 50, t = 33.95, $p < 0.0001$) were highly significant. In addition, the paired t-test of credible interval widths between Hill-MCMC and Linear-bootstrap methods was significant (Figure 7B, n = 50, t = 3.67, p = 0.0006), underscoring the distinction between accuracy and precision.

When applied to experimental anti-AAV9 antibody data, the two statistical approaches again gave similar central estimates that differed systematically from the non-statistical values, confirming their consistency on real measurements (Figure 7C).

Statistical significance does not always imply biological relevance. To bridge this gap, I analyzed the distribution of credible interval widths across a diverse set of serum samples (Figure 7F). I found that 90% of Hill-MCMC intervals were narrower than 0.3 $\log_2$ units (~23% difference on the linear scale). I therefore adopted this value as a data-driven practical equivalence threshold for ND50 comparisons.

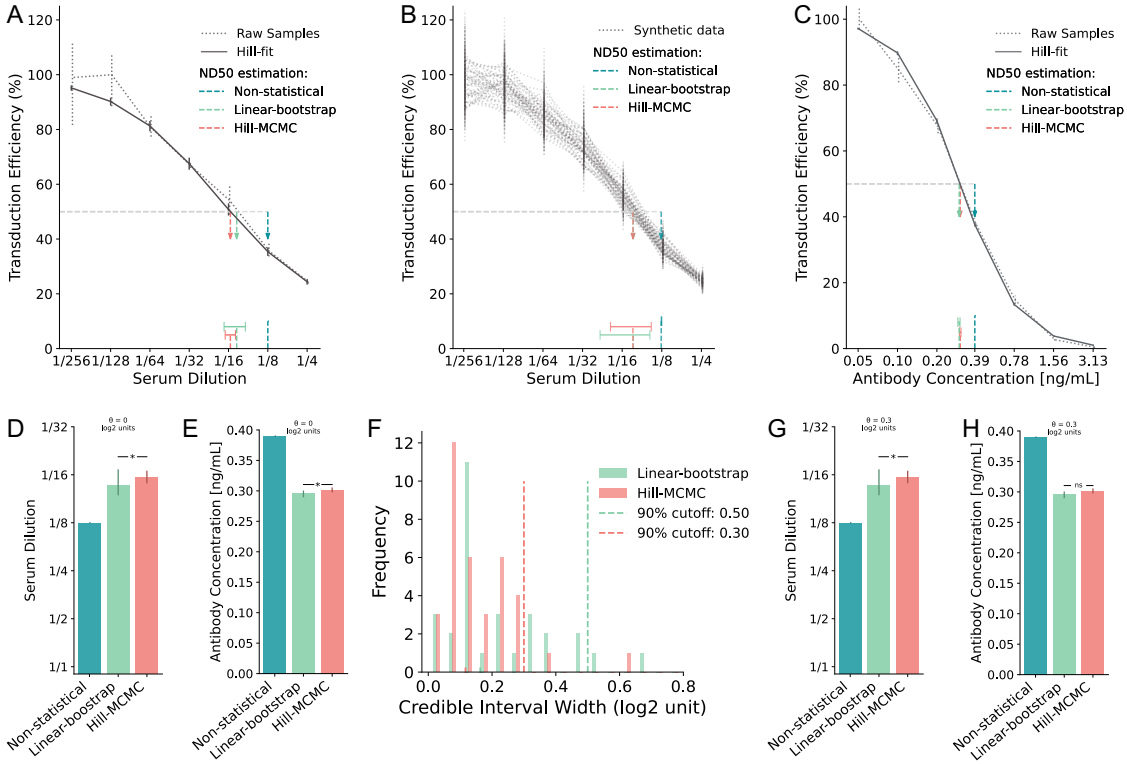

Figure 7. Statistical framework for estimating 50% inhibition.

(A-B) *Estimating 50% inhibition from simulated AAV neutralization assay data (coefficient of variation (CV) = 10%, true 50% inhibition set to 1/16).* ***(A)*** *Neutralization curve with 50% inhibition estimated using three methods: Non-statistical (dilution below 50% mean response threshold), Linear-bootstrap, and Hill-MCMC. The dotted grey curve represents the mean of raw samples, while the solid grey curve shows the Hill-fit model. Vertical, dotted error bars indicate the 95% confidence interval for raw sample means, and the vertical solid error bars indicate the 95% credible intervals for Hill-MCMC fits. Dashed vertical arrows (teal, green, and orange) denote the ND50 estimates, with horizontal bars representing the corresponding uncertainty for the Linear-bootstrap*

and Hill-MCMC methods. ***(B)*** *Mean neutralization curves for 50 synthetic datasets (grey dotted curves), each with random noise (true ND50 set to 1/16). Dashed vertical arrows indicate the mean 50% inhibition estimates with each method. Horizontal bars represent the 95% confidence intervals of ND50 credible interval estimates (CI-of-CIs, Methods). The width of the interval is significantly smaller when the Hill-MCMC method is used.* ***(C)*** *Neutralization curve obtained using coreTIA with an ADK9 antibody dose series. Visual elements represent the same concepts as on (A).* ***(D-E)*** *Comparison of 50% inhibition estimates. Vertical error bars represent the credible intervals for the Linear-bootstrap and Hill-MCMC methods. No error bar is shown for the Non-statistical method, as it yields only a single point estimate. (D) corresponds to synthetic data with a known true ND50, shown on (A). (E) corresponds to data shown on (C) with no known ground truth. A Bayesian threshold test with $\theta = 0$ indicates strong evidence that the estimates differ, with the Hill-MCMC estimate being closest to the true 50% inhibition level. Here, $\theta = 0$ tests whether the difference in ND50 estimates is zero vs. non-zero. A posterior probability >0.95 that the difference is non-zero indicates they differ significantly.* ***(F)*** *Distribution of credible interval widths (log2 units) for pooled assay runs (human, n=33; macaque, n=35). Vertical dashed lines mark the 90th percentile thresholds for Linear-bootstrap (brown, ~0.50 log2 units) and Hill-MCMC (pink, $\theta = 0.3$ log2 units). For comparing ND50 estimates with Hill-MCMC, its 90th percentile ($\theta = 0.3$ log2 units) is adopted as the practical equivalence cutoff, meaning ND50 estimates differing by less than this value are considered effectively equivalent.* ***(G-H)*** *Application of the practical equivalence threshold ($\theta = 0.3$ log2 units) to ND50 comparisons from panels (A) and (C), respectively. (G) ND50 estimates with Linear-bootstrap and Hill-MCMC methods remain significantly different for synthetic data with CV=10%. (H) For ADK9 data (CV=0.027 at 0.2 ng/mL), ND50 estimates differ by less than the threshold (marked "ns" for not significant), indicating practical equivalence despite statistical significance at $\theta = 0$. Asterisks ("*") denote differences exceeding the threshold.*

Applying this threshold showed that, under typical conditions, both statistical methods yielded ND50 estimates that differ from the conventional non-statistical estimates by more than this practically relevant margin (Figure 7G). In contrast, for the low-variability ADK9 dataset, Hill-MCMC and Linear-bootstrap agreed within the 0.3 $\log_2$ window

despite formal statistical differences, indicating that in high-quality datasets the two statistical approaches are practically interchangeable (Figure 7H).

Together, these results emphasize the importance of considering both statistical significance and practical relevance when comparing ND50 estimates. While Linear-bootstrap and Hill-MCMC perform similarly under optimal conditions, the Hill-MCMC model offers improved precision and flexibility, particularly in scenarios with noisier data or incomplete dilution series, which are addressed in the following sections.

4.2.2 Robust ND50 estimation from incomplete dilution series

Designing a robust total inhibition assay requires choosing a dilution scheme that covers the anticipated ND50 range, which can be broad due to pre-existing immunity (e.g. prior AAV exposure) and inter-individual variability in response. In practice, the number of dilution points and technical replicates must be balanced against constraints on cost, complexity and sample volume - particularly in settings where material is limited, such as pediatric studies. Fewer dilution points increase the chance that the true ND50 falls outside the tested range, whereas fewer technical replicates directly reduce the precision and robustness of ND50 estimation, especially for non-model-based methods that are more susceptible to noise (Figure 8). At the opposite extreme, using many dilutions and replicates (e.g. N≥2 at each dilution) improves coverage and precision but increases serum consumption, workload and cost, raising practical and ethical concerns.

To systematically explore this trade-off, I examined whether a Hill-MCMC model could still provide informative ND50 estimates, with quantified uncertainty, when the experimental dilutions do not fully bracket the 50% inhibition point. To this end, I generated 90 noisy neutralization curves with a true ND50 of 1/32 but restricted the sampled dilutions to 1/4, 1/8 and 1/16, deliberately excluding the true ND50. These synthetic data were then grouped into virtual assay runs with three, two or one technical replicate(s) per dilution (Figure 8A; teal = 1, green = 2, orange = 3 replicates), yielding 30 ND50 estimates for each condition.

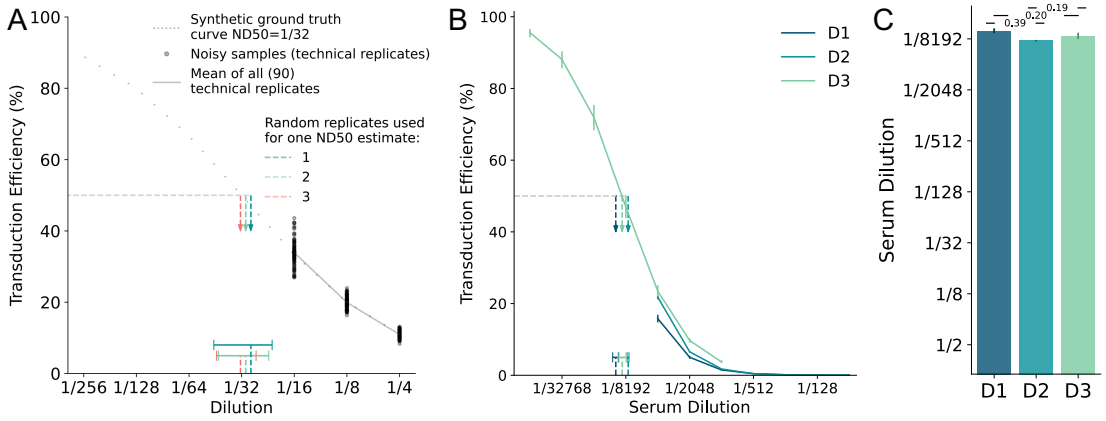

Figure 8. Hill-MCMC Estimation of ND50 with Uncertainty When Dilution Series Do Not Bracket the 50% Inhibition Point.

(A) *Precision of ND50 estimation during extrapolation using synthetic data. The dotted gray curve represents the synthetic ground truth (ND50 = 1/32). Grey dots show examples of noisy measurements (CV = 10%) sampled only at dilutions 1/4, 1/8, and 1/16. The solid grey line represents the mean of all 90 noisy samples. Colored vertical dashed arrows show the posterior mean ND50 estimates derived via Hill-MCMC using 1 (teal), 2 (green), or 3 (orange) randomly chosen technical replicates from the 90 available noisy curves (legend indicates grouping for one example estimate). Horizontal bars at the bottom represent the composite 95% CI-of-CIs intervals (Methods) across 30 independent simulations for each replicate condition, illustrating improved precision (narrower intervals) with more replicates.* ***(B)*** *Hill-MCMC extrapolation applied to real neutralization data. Curves show results from one mouse serum sample tested on different days with different dilution ranges: Day 1 (D1, blue) and Day 2 (D2, teal) used dilutions (1/64–1/4096) that did not bracket the 50% inhibition point, while Day 3 (D3, green) used an adjusted range (1/1024–1/65536) that did. Points show technical replicate means; solid lines show Hill-MCMC fits. Vertical dashed arrows indicate the posterior mean ND50 estimates derived via Hill-MCMC, with horizontal bars representing the corresponding 95% credible intervals. Note the extrapolation required for D1 and D2.* ***(C)*** *Comparison of posterior ND50 estimates across days. Bars represent the posterior mean ND50 estimates derived via Hill-MCMC for Day 1 (D1), Day 2 (D2), and Day 3 (D3). Error bars represent the 95% credible intervals. Numerical annotations indicate the difference (in log2 units) between the posterior means for the indicated comparisons (e.g., D1 vs D3 ≈ 0.19 log2 units).*

Mean ND50 estimates were broadly comparable between three and two replicates ($t = -1.63$, $p = 0.11$) and between two and one replicate ($t = -1.09$, $p = 0.29$), with only a modest but significant shift between three and one replicate ($t = -2.67$, $p = 0.01$). More importantly, the width of the composite uncertainty intervals ("CI-of-CIs") differed substantially across conditions: precision improved consistently as the number of technical replicates increased. CI-of-CIs were narrowest with three replicates and progressively wider with two replicates ($t = 2.08$, $p = 0.046$) and with a single replicate (versus three replicates: $t = -16.77$, $p < 0.0001$; versus two replicates: $t = -23.92$, $p < 0.0001$). These CI-of-CIs therefore capture how both experimental noise and the estimation procedure contribute to overall uncertainty when ND50 must be inferred from limited replicate data.

Taken together, these simulations show that Hill-MCMC can extrapolate ND50 beyond the measured dilution range, but that the precision of such extrapolated estimates depends on the number of technical replicates. From a practical assay-design perspective, the results suggest that at least two technical replicates should be included whenever ND50 is likely to lie outside the tested dilutions.

To illustrate Hill-MCMC extrapolation in an experimental setting, I performed coreTIA measurements on a mouse serum sample across three separate days (Figure 8B, C). This design introduced typical inter-assay variability and did not rely on a shared reference standard, reflecting typical experimental constraints. On days 1 and 2 (D1, D2), the dilution range (1/64–1/4096) did not reach the 50% neutralization point (~1/8192), whereas on day 3 (D3) an adjusted dilution scheme (1/1024–1/65536) fully bracketed ND50. For D1 and D2, non-statistical and Linear-bootstrap methods could not report ND50 because the 50% inhibition point lay outside the sampled range, but Hill-MCMC still produced ND50 estimates with 95% credible intervals by extrapolation. The differences between the extrapolated ND50 values (D1, D2) and the bracketed estimate from D3 were ~0.19 and ~0.20 $\log_2$ units, respectively, which fall within the 0.3 $\log_2$ practical equivalence threshold established earlier. The difference between D1 and D2 (0.39 $\log_2$ units) likely reflects the combined effect of inter-assay variation and extrapolation uncertainty.

By providing full posterior distributions and credible intervals rather than single point estimates or failed fits, the Hill-MCMC approach allows researchers to explicitly assess

the reliability of ND50 values derived from suboptimal dilution series. This capability offers an advantage over methods that either cannot handle out-of-range neutralization or return point estimates without any measure of reliability.

4.3 Comparative validation of the optimized core assay across human and animal models.

4.3.1 Enhanced sample stratification with the CSC design

Building on the advances in assay sensitivity and quantitative analysis, I next examined the practical consequences of coreTIA for stratification of seronegative and seropositive samples. Since accurate discrimination of these sample types underpins both reference pool construction and patient eligibility for AAV gene therapy, understanding how the assay design influences classification outcomes is essential.

Several studies assessing anti-AAV NAb prevalence in human populations have relied on the VSC assay design (17,18,52–54), where total serum content changes across the dilution series. The results presented earlier demonstrate that the CSC-based coreTIA stabilizes baseline transduction and enhances sensitivity compared with the conventional design. To assess how these methodological improvements translate into subject stratification, I analyzed a cohort of 46 human serum samples tested against three AAV capsids (AAV1, AAV5, AAV9) using both VSC and CSC assay formats.

First, I aimed to identify truly seronegative sera suitable for use as an antibody-free control or background matrix (32,54–58). For this purpose, I applied a stringent threshold of >90% transduction at a 1/4 serum dilution. Samples yielding transduction above this threshold were labeled seronegative, while those below were considered "ineligible" for inclusion in a hypothetical reference serum pool (Figure 9A-C). This conservative cutoff minimizes the risk of including low-level neutralizing antibodies (false negatives), aligning with clinical evidence that even trace immunity can impact gene therapy efficacy (33). Furthermore, this stringent cutoff aligns with practices in pseudovirus neutralization assays that employ both 50% and 90% neutralization thresholds for complementary applications (34,59).

The results revealed a striking difference in classification sensitivity. The CSC assay identified significantly more samples as "ineligible" (i.e., containing low-level antibodies) than the VSC format across all tested capsids. Specifically, discordant

classification rates were 30.4% for AAV1, 47.8% for AAV5, and 41.3% for AAV9 ($p < 0.001$ for all comparisons). These findings indicate that the conventional VSC assay frequently fails to detect low-level neutralizing activity, potentially compromising the quality of reference materials used for assay validation, and ultimately patient eligibility determinations.

Next, I re-evaluated the same cohort using the standard clinical criterion: 50% transduction at a 1/4 dilution to distinguish neutralizing from non-neutralizing samples (Figure 9D-E). Under this less stringent threshold, the CSC format still reclassified a substantial proportion of samples that were deemed non-neutralizing by the VSC assay. The discordance was serotype-dependent: while minimal for AAV1 (4.3%, $p = 0.50$), it was statistically significant for AAV5 (15.2%, $p = 0.02$) and AAV9 (21.7%, $p < 0.01$). This variation likely reflects the differential magnitude of serum-induced transduction enhancement observed across serotypes (Figure S1).

These results demonstrate that the CSC-based coreTIA protocol minimizes the confounding effects of variable serum content, preventing the masking of neutralizing activity by matrix-driven enhancement. By providing a more accurate assessment of serostatus, the CSC format improves the reliability of patient stratification, reducing the risk of false-negative classifications that could compromise gene therapy safety and efficacy.

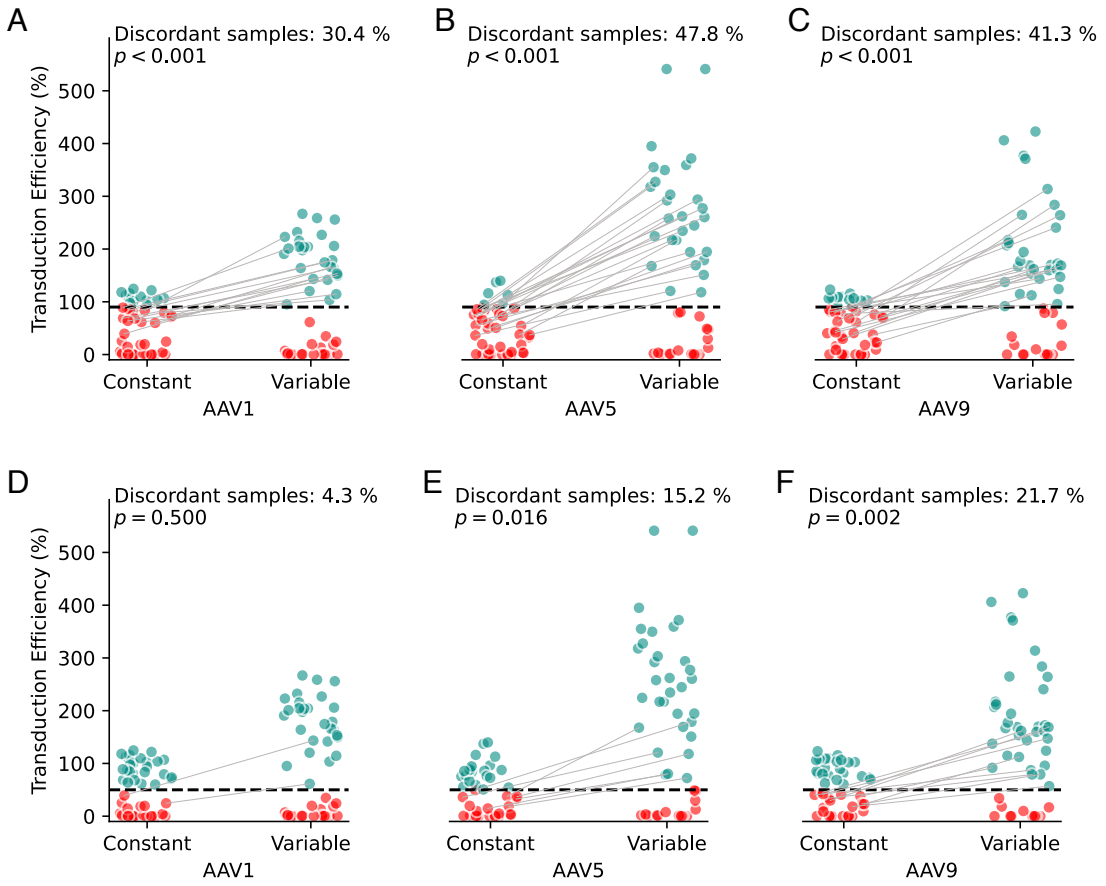

Figure 9. Constant serum concentration (CSC) assay provides more consistent subject stratification than the variable serum concentration (VSC) assay format.

Throughout the figure, Constant refers to the CSC method where total serum remains fixed at 10%, while Variable refers to the VSC method where total serum concentration increases with less dilution. ***(A-C)*** *Identification of putative seronegative samples from a cohort of 46 sera using CSC and VSC assays. Sera yielding above 90% transduction at a 1/4 serum dilution are labeled as seronegative (teal dots), while sera below this threshold are labeled as ineligible for inclusion in a hypothetical reference serum pool (red dots). The black dashed line represents the 90% transduction threshold. The CSC approach assigns more samples as ineligible than the VSC format, reducing misclassification of borderline neutralizers.* ***(D-F)*** *Classification of the same sera into non-neutralizing (teal dots) or neutralizing (red dots) categories using 50% transduction at a 1/4 dilution as criterion. Samples above the black dashed line (50% transduction threshold) are classified as non-neutralizing, whereas those below it are classified as neutralizing. Discordant samples – those classified differently under CSC vs. VSC – are connected by*

gray lines. The proportion of discordant samples is indicated above each plot, with p-values from McNemar tests reflecting the significance of classification differences across AAV serotypes.

4.3.2 Improved performance of the CSC design generalizes across species

New therapies typically progress through a preclinical validation pipeline, which includes both *in vitro* and *in vivo* models. Beyond improving stratification of human sera, establishing a consistent methodology across species is essential for reliable translational comparisons (31). To determine whether the baseline stabilization and enhanced sensitivity of the CSC format extend beyond human samples, I tested sera from two key preclinical species: domestic cats (n=4) and rhesus macaques (n=2) (Figure 10).

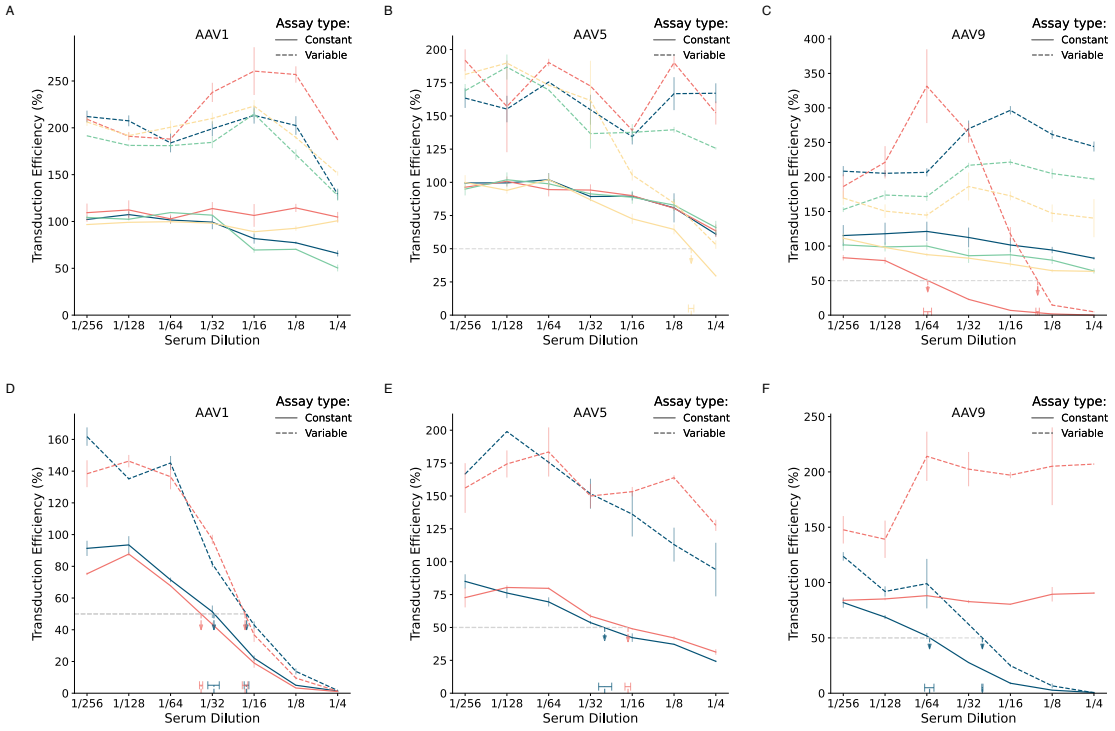

Figure 10. Performance gain of CSC assay generalizes to preclinical model species. *Throughout the figure, Constant refers to the CSC method where total serum remains fixed at 10%, while Variable refers to the VSC method where total serum concentration increases with less dilution. Transduction curves for sera sampled from preclinical subjects tested against three AAV serotypes (AAV1, AAV5, AAV9). Panels **(A-C)** show data from cats (n=4), while Panels **(D-F)** show data from rhesus macaques (n=2). Each color represents an individual subject within each species; same color denotes same*

subject across panels. Solid curves indicate results from the Constant assay, while dashed curves represent results from the Variable assay. Vertical error bars indicate standard deviations from the mean. The horizontal gray dashed line at 50% transduction efficiency indicates the neutralization threshold. For samples that cross below this threshold, ND50 dilutions are marked by colored vertical dashed arrows pointing to horizontal bars that denote 95% credible intervals for the ND50 estimates. Samples without arrows did not reach 50% neutralization within the tested dilution range. The x-axis represents 2-fold serum dilutions, while the y-axis shows transduction efficiency as a percentage of antibody-free controls.

Consistent with human data, sera analyzed with the conventional VSC protocol showed elevated baseline transduction levels across all tested serotypes (AAV1, AAV5, AAV9) in both species (Figure 10, dashed curves). This confirms that matrix-induced enhancement is a cross-species phenomenon. In contrast, the CSC format stabilized baselines near 100% transduction at high dilutions (solid curves), eliminating the artifactual signal boost.

To quantify this improvement, I calculated the effect size between the two assay formats. The difference was maximal, yielding a Cliff's delta of 1.0 (95% CI [1.0, 1.0]), indicating that CSC transduction values were consistently lower (i.e., less inflated) than VSC values across all dilutions, serotypes, and species.

Although sample availability was naturally limited, these results indicate that the benefits of the coreTIA framework are not unique to human serum. The ability to mitigate matrix effects in feline and non-human primate samples supports the utility of CSC-based coreTIA as a robust, harmonized platform for translational research, facilitating more accurate comparison of neutralizing antibody responses from preclinical development to clinical application.

4.3.3 Seroreversion models demonstrate the utility of CSC design in determining neutralizing antibody persistence

Patients often undergo seroreversion, transitioning from a seropositive to a seronegative state following natural exposure to AAV or prior AAV injections (60). Determining this status is a prerequisite for establishing the appropriate timing for re-administration. To evaluate how assay sensitivity influences the detection of antibody persistence, I tested

two preclinical feline models representing distinct immune scenarios: vaccination-induced immunity and immunity acquired via direct AAV injection.

First, I modeled acquired immunity using a standard veterinary vaccination protocol known to induce cross-reactive AAV neutralization (9) (Methods, Figure 11A–B). Serum samples were collected from a subject at two weeks and four months post-vaccination. At both time points, the VSC assay exhibited substantially elevated baseline transduction levels compared to the CSC design, indicating a matrix-driven masking effect. Crucially, while the VSC assay suggested near-complete loss of neutralizing activity by four months (ND50 < 1/4), the CSC format continued to detect significant neutralization (ND50 ≈ 1/8). This discrepancy illustrates that the conventional VSC method risks classifying subjects as seroreverted prematurely, potentially leading to unsafe re-dosing decisions.

Next, I examined the persistence of neutralizing antibodies following direct AAV administration by testing serum samples collected from one cat at one, two, and three years after administration of CAP-B22 (Figure 11C–F).

When tested against the injected vector (CAP-B22), the CSC assay detected neutralizing activity even three years post-injection (ND50 ~ 1/6). In contrast, the VSC assay showed markedly lower neutralization levels at years one and two, and failed to detect any neutralization by year three. A similar pattern emerged when testing against AAV9 (the parental capsid). While both assays captured the expected decline in cross-neutralization over time, the CSC format maintained detection of activity at year two (ND50 ~ 1/12), whereas the VSC format showed only minimal inhibition. This earlier decline in cross-neutralization likely reflected epitope differences between CAP-B22 and AAV9 (41).

These longitudinal observations provide insights into antibody persistence, revealing that neutralizing activity can remain detectable for significantly longer periods than suggested by conventional assays. Although the sample size was necessarily limited by the challenges of long-term large animal studies, the consistent enhancement in sensitivity achieved by the CSC format has direct clinical implications. By preventing the premature declaration of seronegativity, the coreTIA framework supports safer and more accurate determination of eligibility windows for AAV re-administration.

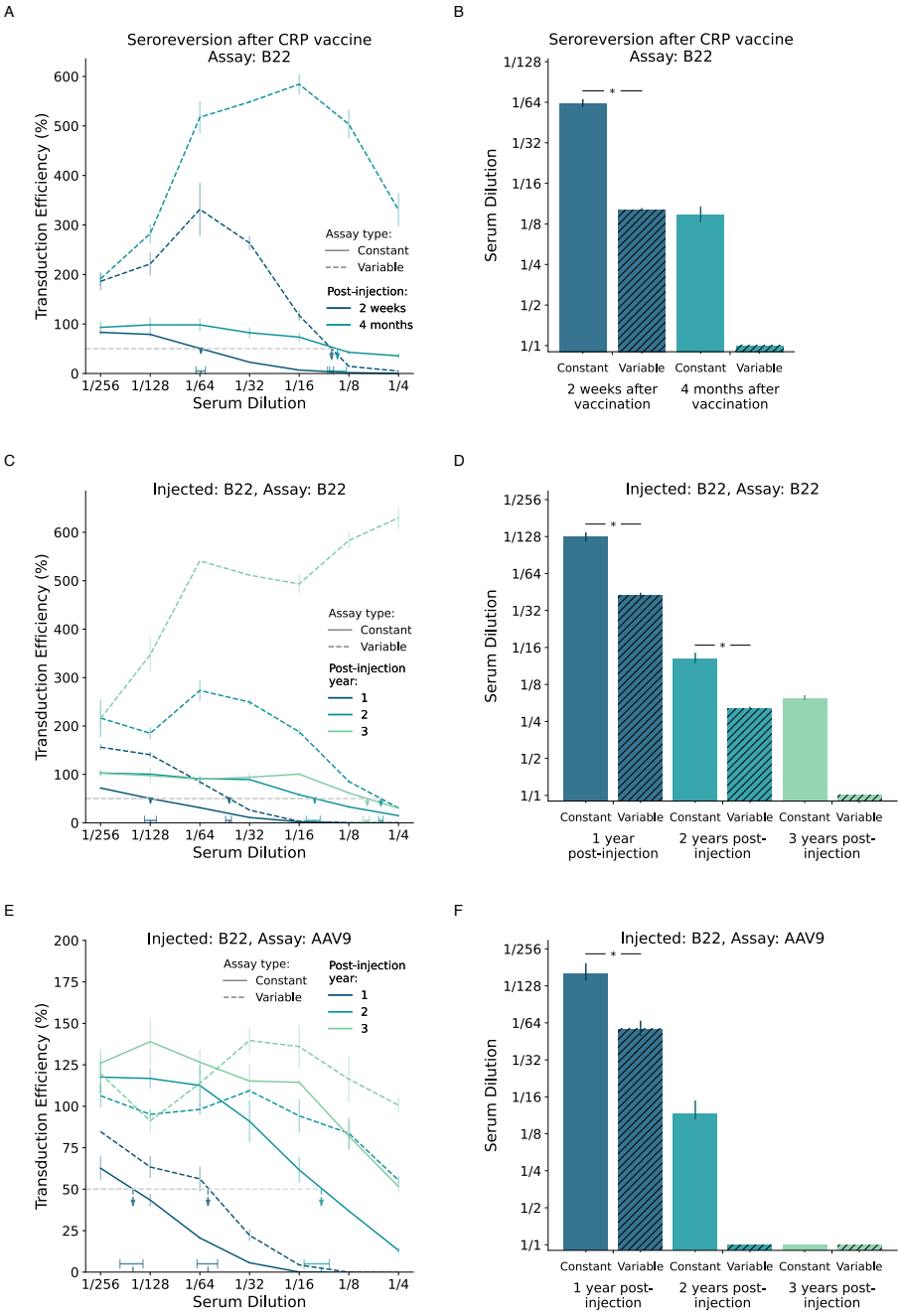

Figure 11. Performance of CSC assay in preclinical seroreversion models

Throughout the figure, Constant refers to the CSC method where total serum remains fixed at 10%, while Variable refers to the VSC method where total serum concentration increases with less dilution. ***(A, C, E)*** *Transduction curves for serum samples collected from preclinical subjects at various time points post-vaccination or post-injection. Solid curves represent results from the Constant assay, dashed curves represent results from the Variable assay. Vertical error bars indicate standard deviations from the mean. The*

horizontal gray dashed line at 50% transduction efficiency indicates the neutralization threshold. ND50 dilutions are marked by colored vertical dashed arrows pointing to horizontal bars that denote 95% credible intervals for ND50 estimates. ***(B, D, F)*** *ND50 estimates derived from the transduction curves in Panels A, C, and E. ND50 values are shown for both Constant (filled bars) and Variable (striped bars) assays at corresponding time points. Error bars represent 95% credible intervals. Asterisks denote significant difference (Methods). For samples exhibiting minimal (ND50 < 1/4) or no neutralization, 1/1 dilution is used as placeholder.* ***(A–B)*** *Serum samples collected from one cat two weeks and four months after vaccination with a feline CRP vaccine. Constant detected persistent neutralizing activity at four months post-vaccination, while Variable reported seroreversion earlier.* ***(C–D)*** *Serum samples collected from one cat one, two, and three years after injection with CAP-B22 capsid. Constant detected persistent seropositivity three years post-injection, whereas Variable suggested seroreversion had occurred by year three.* ***(E–F)*** *Same serum samples as in (C-D) tested against the parental capsid of CAP-B22, AAV9. Seroreversion occurred one year earlier with AAV9 compared to CAP-B22 likely due to limited cross-reactivity between capsids.*

5 Discussion

Accurate quantification of pre-existing neutralizing antibodies is central for safe and effective AAV gene therapy. Despite its importance, neutralization assays are not fully standardized, which leading to discordant results across laboratories and complicating the interpretation of clinical data. In this work, I addressed two key limitations of current assays: the confounding influence of serum matrix effects and the lack of uncertainty quantification. By developing the coreTIA framework – combining the Constant Serum Concentration (CSC) assay design with a Bayesian statistical pipeline – I have established a robust platform that enhances both the sensitivity and reliability of NAb testing.

5.1 Overcoming Matrix Effects for Enhanced Sensitivity

The systematic evaluation of assay parameters demonstrated that conventional Variable Serum Concentration (VSC) assays are affected by a dilution-dependent artifact: baseline transduction increases as serum is diluted. My data showed that serum components exert a dual effect – enhancing transduction when pre-incubated with viral particles but inhibiting it when applied directly to cells. In VSC protocols, as the serum is diluted out, the total protein content drops, progressively altering the cellular environment and amplifying this artifactual enhancement. This "baseline drift" compresses the assay's dynamic range and effectively masks partial neutralization, leading to false-negative results.

The Constant Serum Concentration (CSC) format resolves this issue by maintaining a constant serum environment across all dilution steps. By diluting the test serum with fetal bovine serum (FBS), baseline transduction remained near 100% for non-neutralizing samples. This reduced matrix-driven enhancement and revealed neutralizing activity that would otherwise be missed, increasing ND50 estimates and improving detection at lower antibody levels compared with VSC. These gains did not require additional procedural complexity, making CSC suitable for higher-throughput screening.

5.2 The Necessity of Uncertainty Quantification

Beyond addressing shortcomings in assay biochemistry, this work highlights the importance of statistical rigor in NAb assessment. Commonly used threshold-based methods, which reduce complex dose-response data to a single point estimate, fail to

convey the reliability of the measurement. This is particularly problematic in pediatric studies or retrospective analyses where sample availability is limited, often precluding extensive replication.

The Bayesian statistical framework integrated into coreTIA addresses this gap by providing credible intervals for every ND50 estimate. My comparison of Linear-bootstrap and Hill-MCMC methods revealed that while both improve upon non-statistical approaches, the Hill-MCMC model provides greater precision and flexibility. A key advantage of this model is its ability to extrapolate ND50 values with quantified uncertainty even when the dilution series does not fully bracket the 50% inhibition point. This capability prevents data loss and reduces the need for repeat testing, conserving limited biological samples. Furthermore, by establishing a practical equivalence threshold based on empirical assay variability, I provided a framework for distinguishing meaningful biological differences from technical noise, preventing the over-interpretation of minor fluctuations in NAb level.

5.3 Clinical Implications for Patient Stratification and Safety

The enhanced sensitivity and reliability of the coreTIA platform have direct implications for patient safety. Misclassification of serostatus is a major risk in gene therapy; even low antibody levels can compromise transduction efficacy and long-term gene expression (14,28).

My analysis of human serum cohorts demonstrated that the CSC assay reclassified a substantial proportion of samples – up to 21.7% for AAV9 – from "non-neutralizing" to "neutralizing" compared to the VSC format. These borderline samples, which fall near clinical cutoffs, represent patients who might be misclassified as eligible for treatment using less sensitive assays, potentially placing them at risk of immune-mediated therapeutic failure. By identifying these low-level responses, the CSC design supports more accurate risk stratification and enables informed decisions regarding vector dosing or prophylactic immune suppression in specific patient subgroups.

5.4 Insights into Antibody Persistence and Seroreversion

Accurate monitoring of immune responses over time is essential for determining the window for potential re-administration. My longitudinal studies in feline models showed

that conventional assays may prematurely declare seroreversion (the loss of detectable immunity).

In the vaccination-induced immunity model, the VSC assay indicated a loss of neutralization by four months, whereas the CSC format continued to detect activity. Similarly, in the AAV-injected model, the CSC assay detected persistent neutralization against the capsid even three years post-administration – one year after the VSC assay signal had faded. These findings suggest that patients may remain seropositive for significantly longer periods than currently estimated. This has profound implications for multi-dose therapies (e.g., for Duchenne muscular dystrophy) (2), where premature re-dosing could lead to rapid vector clearance and adverse immune reactions.

5.5 Limitations and Future Directions

Beyond clinical applications, the coreTIA framework is particularly relevant for basic neuroscience research utilizing non-human primate models. Given the high ethical and financial cost of primate studies, accurate screening for pre-existing immunity against CNS-targeting vectors is essential to prevent confounding by unrecognized immunity and ensure efficient resource use. This is especially critical when testing novel synthetic capsids designed for CNS delivery, where unexpected immune interactions can confound experimental outcomes.

While coreTIA improves assay sensitivity and reliability, certain limitations warrant further investigation. First, the empty-to-full capsid ratio of AAV preparations is a known variable influencing assay sensitivity, as empty capsids can act as decoys for neutralizing antibodies (61–63). Although I controlled for this by using shared viral batches for all comparative experiments, future standardization efforts should incorporate well-characterized vector reference standards to enhance inter-laboratory comparability (64).

Second, while the principles of the CSC design are broadly applicable, their generalizability to other viral vectors remains to be empirically tested. Serum matrix effects are known to influence infectivity and antibody binding across various viral systems (56). Future studies should explore whether similar matrix-stabilization strategies can improve the reliability of neutralization assays in vaccine development and immune monitoring for other infectious diseases.

Finally, the ultimate validation of any *in vitro* assay lies in its predictive value for clinical outcomes (31). Variable therapeutic outcomes have been reported in animal models

classified as having similar serostatus by conventional assays, with several studies identifying inconsistent treatment responses (37,65). This variability suggests that conventional assays may fail to capture subtle but biologically significant differences in neutralizing activity. Future work should therefore focus on correlating CSC-derived ND50 values with *in vivo* transgene expression in large animal models or clinical trials. Establishing such a correlation would confirm the utility of coreTIA not just as an analytical tool, but as a predictive biomarker for therapeutic success, potentially resolving the discrepancies observed in earlier preclinical studies.

6 Conclusions

AAV vectors have become indispensable tools in basic neuroscience, enabling precise circuit mapping, optogenetic manipulation, and the treatment of neurological disorders. However, the successful application of these tools – both in translational neuroscience and clinical neurology – is often hindered by pre-existing immunity. The primary aim of my work was to establish a harmonized method for quantifying AAV neutralizing antibodies to improve the applicability of these interventions. By resolving critical measurement discrepancies, my work enhances patient stratification for gene therapy and supports translational research. The major scientific contributions and new results of my thesis are summarized below:

Thesis I: Elimination of matrix effects via the Constant Serum Concentration (CSC) design

- I demonstrated that conventional AAV neutralization assays suffer from a systematic artifact – dilution-dependent baseline inflation – caused by variable serum content.
- I showed that maintaining a constant serum concentration (a central element of the coreTIA protocol) stabilizes assay baselines and unmasks neutralizing activity that is otherwise obscured by matrix effects.
- I showed that this optimized experimental design increases sensitivity without compromising procedural simplicity.

Thesis II: Establishment of a Bayesian statistical framework for robust NAb quantification

- I integrated a statistical workflow into the coreTIA framework, implementing the Linear-bootstrap and Bayesian Hill-MCMC approaches to quantify the uncertainty of every ND50 estimate.
- I demonstrated that the Hill-MCMC model provides superior performance: it yields narrower credible intervals than linear interpolation and allows for the estimation of ND50 values even when the 50% inhibition point lies outside the measured dilution range.

- I established a data-driven "practical equivalence" threshold (0.3 $\log_2$ units), providing a quantitative criterion to distinguish meaningful biological differences from technical assay variability.

Thesis III: Enhanced patient stratification and long-term immune monitoring

- I validated the clinical and translational utility of the coreTIA framework across human and animal cohorts including feline and rhesus macaque subjects, which are key models for translational neuroscience.
- I showed that coreTIA reclassifies a significant proportion of human samples as seropositive that were deemed seronegative by conventional methods, thereby reducing the risk of false-negative patient stratification.
- I found through longitudinal feline models that neutralizing antibodies persist for longer periods (up to 3 years) than detected by conventional assays. This finding provides important data for determining the timing of potential re-administration and demonstrates coreTIA's improved performance in monitoring long-term immune responses.

My thesis resolves a methodological bottleneck in neurological gene therapy. By enabling reliable quantification of immunity against both standard serotypes and novel synthetic capsids engineered for the nervous system, coreTIA supports the planning of translational studies and improves the safety assessment of gene therapies for CNS disorders.

7 Summary

Adeno-associated virus (AAV) vectors are currently the leading platform for *in vivo* gene therapy. However, the widespread prevalence of pre-existing neutralizing antibodies (NAbs) against the AAV capsid in the human population poses a barrier to safety and efficacy. Consequently, sensitive and reliable screening of patients prior to treatment is essential. Despite this need, the currently used neutralization assays lack standardization and are often limited by two factors: the "serum matrix effect," where variable serum components artificially enhance viral transduction and mask low-level antibodies; and the lack of a consistent statistical framework, which often leads to subjective data interpretation.

To address these limitations, my doctoral thesis introduces coreTIA (core Transduction Inhibition Assay), a comprehensive framework that integrates an optimized experimental protocol with a rigorous statistical pipeline.

The experimental foundation of coreTIA is the Constant Serum Concentration (CSC) design, which maintains a constant serum environment across dilution points. This approach stabilizes assay baselines and unmasks low-level neutralizing activity. The optimization was validated across multiple AAV serotypes (AAV1, AAV5, AAV9) and species, including mice, cats, monkeys and humans.

Complementing the experimental workflow, I developed an open-source statistical framework for objective data analysis. Utilizing a Bayesian probabilistic model, this pipeline enables the precise estimation of 50% neutralizing dose (ND50) and quantifies measurement uncertainty, offering an alternative to subjective manual evaluation.

The sensitivity of the coreTIA platform was demonstrated by identifying pre-existing immunity in up to 21.7% of human samples that were classified as "seronegative" by conventional testing. Furthermore, in preclinical seroreversion studies, the assay extended the detection window of persisting antibodies by over a year. In conclusion, this harmonized platform provides a reliable tool for patient stratification, minimizing the risk of false-negative classification and immune-mediated treatment failure in gene therapy.

8 References

1. Wang JH, Gessler DJ, Zhan W, Gallagher TL, Gao G. Adeno-associated virus as a delivery vector for gene therapy of human diseases. Sig Transduct Target Ther. 2024 Apr 3;9(1):1–33. doi:10.1038/s41392-024-01780-w

2. Ling Q, Herstine JA, Bradbury A, Gray SJ. AAV-based in vivo gene therapy for neurological disorders. Nat Rev Drug Discov. 2023 Oct;22(10):789–806. doi:10.1038/s41573-023-00766-7

3. Mendell JR, Al-Zaidy S, Shell R, Arnold WD, Rodino-Klapac LR, Prior TW, et al. Single-Dose Gene-Replacement Therapy for Spinal Muscular Atrophy. New England Journal of Medicine. 2017 Nov 2;377(18):1713–22. doi:10.1056/NEJMoa1706198

4. Nathwani AC, Reiss UM, Tuddenham EGD, Rosales C, Chowdary P, McIntosh J, et al. Long-Term Safety and Efficacy of Factor IX Gene Therapy in Hemophilia B. New England Journal of Medicine. 2014 Nov 20;371(21):1994–2004. doi:10.1056/NEJMoa1407309

5. Chhabra A, Bashirians G, Petropoulos CJ, Wrin T, Paliwal Y, Henstock PV, et al. Global seroprevalence of neutralizing antibodies against adeno-associated virus serotypes used for human gene therapies. Molecular Therapy Methods & Clinical Development. 2024 Sep 12;32(3):3. doi:10.1016/j.omtm.2024.101273 PubMed PMID: 39022744.

6. Kruzik A, Fetahagic D, Hartlieb B, Dorn S, Koppensteiner H, Horling FM, et al. Prevalence of Anti-Adeno-Associated Virus Immune Responses in International Cohorts of Healthy Donors. Molecular Therapy - Methods & Clinical Development. 2019 Sep;14:126–33. doi:10.1016/j.omtm.2019.05.014

7. Wang D, Li M, Li J, Tran K, Ren L, He R, et al. Adeno-Associated Virus Neutralizing Antibodies in Large Animals and Their Impact on Brain Intraparenchymal Gene Transfer. Molecular Therapy - Methods & Clinical Development. 2018 Dec 14;11:65–72. doi:10.1016/j.omtm.2018.09.003

8. Mingozzi F, Chen Y, Edmonson SC, Zhou S, Thurlings RM, Tak PP, et al. Prevalence and pharmacological modulation of humoral immunity to AAV vectors in gene transfer to synovial tissue. Gene Ther. 2013 Apr;20(4):417–24. doi:10.1038/gt.2012.55 PubMed PMID: 22786533; PubMed Central PMCID: PMC3473155.

9. Adachi K, Dissen GA, Lomniczi A, Xie Q, Ojeda SR, Nakai H. Adeno-associated virus-binding antibodies detected in cats living in the Northeastern United States lack neutralizing activity. Sci Rep. 2020 Jun 22;10(1):1. doi:10.1038/s41598-020-66596-4

10. Tseng YS, Agbandje-Mckenna M. Mapping the AAV Capsid Host Antibody Response toward the Development of Second Generation Gene Delivery Vectors. Front Immunol. 2014 Jan 30;5. doi:10.3389/fimmu.2014.00009

11. Murphy SL, Li H, Mingozzi F, Sabatino D, Hui D, Edmonson S, et al. Diverse IgG Subclass Responses to Adeno-associated Virus Infection and Vector Administration. J Med Virol. 2009 Jan;81(1):65–74. doi:10.1002/jmv.21360 PubMed PMID: 19031458; PubMed Central PMCID: PMC2782623.

12. Padron E, Bowman V, Kaludov N, Govindasamy L, Levy H, Nick P, et al. Structure of Adeno-Associated Virus Type 4. J Virol. 2005 Apr;79(8):5047–58. doi:10.1128/JVI.79.8.5047-5058.2005 PubMed PMID: 15795290; PubMed Central PMCID: PMC1069529.

13. Fitzpatrick Z, Leborgne C, Barbon E, Masat E, Ronzitti G, Van Wittenberghe L, et al. Influence of Pre-existing Anti-capsid Neutralizing and Binding Antibodies on AAV Vector Transduction. Molecular Therapy - Methods & Clinical Development. 2018 Jun;9:119–29. doi:10.1016/j.omtm.2018.02.003

14. Kotterman MA, Yin L, Strazzeri JM, Flannery JG, Merigan WH, Schaffer DV. Antibody neutralization poses a barrier to intravitreal adeno-associated viral vector gene delivery to non-human primates. Gene Ther. 2015 Feb;22(2):2. doi:10.1038/gt.2014.115

15. Mendell JR, Connolly AM, Lehman KJ, Griffin DA, Khan SZ, Dharia SD, et al. Testing preexisting antibodies prior to AAV gene transfer therapy: rationale, lessons and future considerations. Molecular Therapy - Methods & Clinical Development. 2022 Jun;25:74–83. doi:10.1016/j.omtm.2022.02.011

16. Whitehead M, Osborne A, Yu-Wai-Man P, Martin K. Humoral immune responses to AAV gene therapy in the ocular compartment. Biological Reviews. 2021;96(4):1616–44. doi:10.1111/brv.12718

17. Cao L, Ledeboer A, Pan Y, Lu Y, Meyer K. Clinical enrollment assay to detect preexisting neutralizing antibodies to AAV6 with demonstrated transgene expression in gene therapy trials. Gene Ther. 2023 Feb;30(1–2):1–2. doi:10.1038/s41434-022-00353-2

18. Calcedo R, Vandenberghe LH, Gao G, Lin J, Wilson JM. Worldwide Epidemiology of Neutralizing Antibodies to Adeno-Associated Viruses. J INFECT DIS. 2009 Feb;199(3):3. doi:10.1086/595830

19. Hinderer C, Bell P, Louboutin JP, Zhu Y, Yu H, Lin G, et al. Neonatal Systemic AAV Induces Tolerance to CNS Gene Therapy in MPS I Dogs and Nonhuman Primates. Molecular Therapy. 2015 Aug 1;23(8):8. doi:10.1038/mt.2015.99

20. Bartel M, Schaffer D, Büning H. Enhancing the Clinical Potential of AAV Vectors by Capsid Engineering to Evade Pre-Existing Immunity. Front Microbiol. 2011;2:204. doi:10.3389/fmicb.2011.00204 PubMed PMID: 22065962; PubMed Central PMCID: PMC3207363.

21. Chan YK, Wang SK, Chu CJ, Copland DA, Letizia AJ, Costa Verdera H, et al. Engineering adeno-associated viral vectors to evade innate immune and inflammatory responses. Science Translational Medicine. 2021 Feb 10;13(580):580. doi:10.1126/scitranslmed.abd3438

22. Cheng M, Dietz L, Gong Y, Eichler F, Nammour J, Ng C, et al. Neutralizing Antibody Evasion and Transduction with Purified Extracellular Vesicle-Enveloped Adeno-Associated Virus Vectors. Hum Gene Ther. 2021 Dec 1;32(23–24):1457–70.

doi:10.1089/hum.2021.122 PubMed PMID: 34445894; PubMed Central PMCID: PMC8742275.

23. Elmore ZC, Oh DK, Simon KE, Fanous MM, Asokan A. Rescuing AAV gene transfer from neutralizing antibodies with an IgG-degrading enzyme. JCI Insight. 5(19):e139881. doi:10.1172/jci.insight.139881 PubMed PMID: 32941184; PubMed Central PMCID: PMC7566709.

24. György B, Fitzpatrick Z, Crommentuijn MH, Mu D, Maguire CA. Naturally enveloped AAV vectors for shielding neutralizing antibodies and robust gene delivery in vivo. Biomaterials. 2014 Aug;35(26):7598–609. doi:10.1016/j.biomaterials.2014.05.032 PubMed PMID: 24917028; PubMed Central PMCID: PMC4104587.

25. Leborgne C, Barbon E, Alexander JM, Hanby H, Delignat S, Cohen DM, et al. IgG-cleaving endopeptidase enables in vivo gene therapy in the presence of anti-AAV neutralizing antibodies. Nat Med. 2020 Jul;26(7):1096–101. doi:10.1038/s41591-020-0911-7

26. Li X, La Salvia S, Liang Y, Adamiak M, Kohlbrenner E, Jeong D, et al. Extracellular Vesicle–Encapsulated Adeno-Associated Viruses for Therapeutic Gene Delivery to the Heart. Circulation. 2023 Aug;148(5):405–25. doi:10.1161/CIRCULATIONAHA.122.063759

27. Li X, Wei X, Lin J, Ou L. A versatile toolkit for overcoming AAV immunity. Front Immunol. 2022 Sep 2;13. doi:10.3389/fimmu.2022.991832

28. Mingozzi F, High KA. Immune responses to AAV vectors: overcoming barriers to successful gene therapy. Blood. 2013 Jul 4;122(1):1. doi:10.1182/blood-2013-01-306647

29. Ros-Gañán I, Hommel M, Trigueros-Motos L, Tamarit B, Rodríguez-García E, Salas D, et al. Optimising the IgG-degrading enzyme treatment regimen for enhanced adeno-associated virus transduction in the presence of neutralising antibodies. Clin

Transl Immunology. 2022 Feb 24;11(2):e1375. doi:10.1002/cti2.1375 PubMed PMID: 35228870; PubMed Central PMCID: PMC8867416.

30. Vrellaku B, Sethw Hassan I, Howitt R, Webster CP, Harriss E, McBlane F, et al. A systematic review of immunosuppressive protocols used in AAV gene therapy for monogenic disorders. Mol Ther. 2024 Oct 2;32(10):3220–59. doi:10.1016/j.ymthe.2024.07.016 PubMed PMID: 39044426; PubMed Central PMCID: PMC11489562.

31. Braun M, Lange C, Schatz P, Long B, Stanta J, Gorovits B, et al. Preexisting antibody assays for gene therapy: Considerations on patient selection cutoffs and companion diagnostic requirements. Molecular Therapy Methods & Clinical Development. 2024 Mar 14;32(1):1. doi:10.1016/j.omtm.2024.101217 PubMed PMID: 38496304.

32. Myler H, Pedras-Vasconcelos J, Lester T, Civoli F, Xu W, Wu B, et al. Neutralizing Antibody Validation Testing and Reporting Harmonization. AAPS J. 2023 Jul 8;25(4):4. doi:10.1208/s12248-023-00830-5

33. Schulz M, Levy DI, Petropoulos CJ, Bashirians G, Winburn I, Mahn M, et al. Binding and neutralizing anti-AAV antibodies: Detection and implications for rAAV-mediated gene therapy. Molecular Therapy. 2023 Mar;31(3):3. doi:10.1016/j.ymthe.2023.01.010

34. Gorovits B, Fiscella M, Havert M, Koren E, Long B, Milton M, et al. Recommendations for the Development of Cell-Based Anti-Viral Vector Neutralizing Antibody Assays. AAPS J. 2020 Mar;22(2):2. doi:10.1208/s12248-019-0403-1

35. Jungmann A, Müller O, Rapti K. Cell-Based Measurement of Neutralizing Antibodies Against Adeno-Associated Virus (AAV). Methods Mol Biol. 2017;1521:109–26. doi:10.1007/978-1-4939-6588-5_7 PubMed PMID: 27910044.

36. Rapti K, Louis-Jeune V, Kohlbrenner E, Ishikawa K, Ladage D, Zolotukhin S, et al. Neutralizing Antibodies Against AAV Serotypes 1, 2, 6, and 9 in Sera of Commonly Used Animal Models. Mol Ther. 2012 Jan;20(1):1.

doi:10.1038/mt.2011.177 PubMed PMID: 21915102; PubMed Central PMCID: PMC3255603.

37. Ail D, Ren D, Brazhnikova E, Nouvel-Jaillard C, Bertin S, Mirashrafi SB, et al. Systemic and local immune responses to intraocular AAV vector administration in non-human primates. Molecular Therapy - Methods & Clinical Development. 2022 Mar;24:306–16. doi:10.1016/j.omtm.2022.01.011

38. Gardner MR, Mendes DE, Muniz CP, Martinez-Navio JM, Fuchs SP, Gao G, et al. High concordance of ELISA and neutralization assays allows for the detection of antibodies to individual AAV serotypes. Molecular Therapy - Methods & Clinical Development. 2022 Mar;24:199–206. doi:10.1016/j.omtm.2022.01.003

39. Kaplitt MG, Feigin A, Tang C, Fitzsimons HL, Mattis P, Lawlor PA, et al. Safety and tolerability of gene therapy with an adeno-associated virus (AAV) borne GAD gene for Parkinson's disease: an open label, phase I trial. The Lancet. 2007 Jun;369(9579):9579. doi:10.1016/S0140-6736(07)60982-9

40. Zheng Z, Ye J, Leng M, Gan C, Tang N, Li W, et al. Enhanced sensitivity of neutralizing antibody detection for different AAV serotypes using HeLa cells with overexpressed AAVR. Front Pharmacol. 2023 Apr 27;14:1188290. doi:10.3389/fphar.2023.1188290

41. Goertsen D, Flytzanis NC, Goeden N, Chuapoco MR, Cummins A, Chen Y, et al. AAV capsid variants with brain-wide transgene expression and decreased liver targeting after intravenous delivery in mouse and marmoset. Nat Neurosci. 2022 Jan;25(1):1. doi:10.1038/s41593-021-00969-4

42. Beal J. Biochemical complexity drives log-normal variation in genetic expression. Eng biol. 2017 Jun;1(1):55–60. doi:10.1049/enb.2017.0004

43. Kundert K. Wellmap: a file format for microplate layouts. BMC Research Notes. 2021 May 1;14(1):164. doi:10.1186/s13104-021-05573-0

44. Cliff N. Dominance Statistics: Ordinal Analyses to Answer Ordinal Questions. 1993.

45. Zhang A hua, Sun H, Yan G li, Han Y, Wang X jun. Serum Proteomics in Biomedical Research: A Systematic Review. Appl Biochem Biotechnol. 2013 Jun;170(4):774–86. doi:10.1007/s12010-013-0238-7

46. Rogers GL, Huang C, Clark RDE, Seclén E, Chen HY, Cannon PM. Optimization of AAV6 transduction enhances site-specific genome editing of primary human lymphocytes. Mol Ther Methods Clin Dev. 2021 Sep 10;23:198–209. doi:10.1016/j.omtm.2021.09.003 PubMed PMID: 34703842; PubMed Central PMCID: PMC8517001.

47. Wang M, Sun J, Crosby A, Woodard K, Hirsch ML, Samulski RJ, et al. Direct Interaction of Human Serum Proteins with AAV Virions to Enhance AAV Transduction: Immediate Impact on Clinical Applications. Gene Ther. 2017 Jan;24(1):1. doi:10.1038/gt.2016.75 PubMed PMID: 27834949; PubMed Central PMCID: PMC5269444.

48. Pan Y, Rohde M, Zeitler J, Namburi SVS, Cao L, Hu J, et al. A sensitive AAV transduction inhibition assay assists evaluation of critical factors for detection and concordance of pre-existing antibodies. Molecular Therapy - Methods & Clinical Development. 2023 Dec;31:101126. doi:10.1016/j.omtm.2023.101126

49. Watano R, Ohba K, Sehara Y, Hayashi Y, Saga Y, Urabe M, et al. Limitation of Assay Sensitivity Revealed by the Improvement of Cell-Based Assay Against Various Adeno-Associated Virus Serotypes. Human Gene Therapy. 2025 Jun;36(11–12):914–24. doi:10.1089/hum.2024.261

50. Baatartsogt N, Kashiwakura Y, Hayakawa M, Kamoshita N, Hiramoto T, Mizukami H, et al. A sensitive and reproducible cell-based assay via secNanoLuc to detect neutralizing antibody against adeno-associated virus vector capsid. Molecular Therapy - Methods & Clinical Development. 2021 Sep;22:162–71. doi:10.1016/j.omtm.2021.06.004

51. Wang M, Crosby A, Hastie E, Samulski JJ, McPhee S, Joshua G, et al. Prediction of adeno-associated virus neutralizing antibody activity for clinical application. Gene Ther. 2015 Dec;22(12):12. doi:10.1038/gt.2015.69

52. Boutin S, Monteilhet V, Veron P, Leborgne C, Benveniste O, Montus MF, et al. Prevalence of Serum IgG and Neutralizing Factors Against Adeno-Associated Virus (AAV) Types 1, 2, 5, 6, 8, and 9 in the Healthy Population: Implications for Gene Therapy Using AAV Vectors. Human Gene Therapy. 2010 Jun;21(6):704–12. doi:10.1089/hum.2009.182

53. Konkle BA, Walsh CE, Escobar MA, Josephson NC, Young G, von Drygalski A, et al. BAX 335 hemophilia B gene therapy clinical trial results: potential impact of CpG sequences on gene expression. Blood. 2021 Feb 11;137(6):763–74. doi:10.1182/blood.2019004625 PubMed PMID: 33067633; PubMed Central PMCID: PMC7885820.

54. Pabinger I, Ayash-Rashkovsky M, Escobar M, Konkle BA, Mingot-Castellano ME, Mullins ES, et al. Multicenter assessment and longitudinal study of the prevalence of antibodies and related adaptive immune responses to AAV in adult males with hemophilia. Gene Ther. 2024 May;31(5):273–84. doi:10.1038/s41434-024-00441-5

55. Falese L, Sandza K, Yates B, Triffault S, Gangar S, Long B, et al. Strategy to detect pre-existing immunity to AAV gene therapy. Gene Ther. 2017 Dec;24(12):12. doi:10.1038/gt.2017.95

56. Gorovits B, Azadeh M, Buchlis G, Harrison T, Havert M, Jawa V, et al. Evaluation of the Humoral Response to Adeno-Associated Virus-Based Gene Therapy Modalities Using Total Antibody Assays. AAPS J. 2021 Sep 16;23(6):108. doi:10.1208/s12248-021-00628-3

57. Kruzik A, Koppensteiner H, Fetahagic D, Hartlieb B, Dorn S, Romeder-Finger S, et al. Detection of Biologically Relevant Low-Titer Neutralizing Antibodies Against Adeno-Associated Virus Require Sensitive *In Vitro* Assays. Human Gene Therapy Methods. 2019 Apr;30(2):2. doi:10.1089/hgtb.2018.263

58. Kasprzyk T, Triffault S, Long BR, Zoog SJ, Vettermann C. Confirmatory detection of neutralizing antibodies to AAV gene therapy using a cell-based transduction inhibition assay. Molecular Therapy - Methods & Clinical Development. 2022 Mar;24:222–9. doi:10.1016/j.omtm.2022.01.004

59. D'Apice L, Trovato M, Gramigna G, Colavita F, Francalancia M, Matusali G, et al. Comparative analysis of the neutralizing activity against SARS-CoV-2 Wuhan-Hu-1 strain and variants of concern: Performance evaluation of a pseudovirus-based neutralization assay. Front Immunol. 2022 Sep 26;13. doi:10.3389/fimmu.2022.981693

60. Olden RW van, Bianco CL, Dilly KW, Savelieva M, Xu S, Tijsma A, et al. Adeno-associated virus serotype 9 antibodies in neonates and young children: Seroprevalence and kinetics. Molecular Therapy Methods & Clinical Development. 2024 Dec 12;32(4). doi:10.1016/j.omtm.2024.101344

61. Lock M, Alvira MR, Wilson JM. Analysis of Particle Content of Recombinant Adeno-Associated Virus Serotype 8 Vectors by Ion-Exchange Chromatography. Human Gene Therapy Methods. 2012 Feb;23(1):56–64. doi:10.1089/hgtb.2011.217

62. Mingozzi F, Anguela XM, Pavani G, Chen Y, Davidson RJ, Hui DJ, et al. Overcoming Preexisting Humoral Immunity to AAV Using Capsid Decoys. Science Translational Medicine. 2013 Jul 17;5(194):194ra92-194ra92. doi:10.1126/scitranslmed.3005795

63. Aronson SJ, Veron P, Collaud F, Hubert A, Delahais V, Honnet G, et al. Prevalence and Relevance of Pre-Existing Anti-Adeno-Associated Virus Immunity in the Context of Gene Therapy for Crigler–Najjar Syndrome. Human Gene Therapy. 2019 Oct;30(10):1297–305. doi:10.1089/hum.2019.143

64. McColl-Carboni A, Dollive S, Laughlin S, Lushi R, MacArthur M, Zhou S, et al. Analytical characterization of full, intermediate, and empty AAV capsids. Gene Ther. 2024;31(5–6):285–94. doi:10.1038/s41434-024-00444-2 PubMed PMID: 38374348; PubMed Central PMCID: PMC11090809.

65. Wang L, Calcedo R, Bell P, Lin J, Grant RL, Siegel DL, et al. Impact of Pre-Existing Immunity on Gene Transfer to Nonhuman Primate Liver with Adeno-Associated Virus 8 Vectors. Human Gene Therapy. 2011 Apr 8;22(11):1389. doi:10.1089/hum.2011.031 PubMed PMID: 21476868.

9 Bibliography of the candidate's publications

Publications related to the thesis

Kovács B, Somogyi F, Szabó V, Nagy ZZ, Hernádi I, Mátyás F, Vanduffel W, Szemlaky Z, Rózsa B, Ulbert I, Hillier D. CoreTIA: a modular, statistically robust transduction inhibition assay for AAV neutralization. Front Immunol. 2025;16:1623848. doi: 10.3389/fimmu.2025.1623848.

Kovács B, Szabó V, Horváth D, Dobos AB, Nagy ZZ, Vanduffel W, Szemlaky Z, Szepesi Á, Ulbert I, Rózsa B, Hillier D. Overcoming matrix effects in AAV neutralization assays with a constant serum concentration approach. Gene Ther. 2025. doi: 10.1038/s41434-025-00567-0.

Publications independent of the thesis

Domahidy F, **Kovács B**, Cseri L, Katona G, Rózsa B, Mucsi Z, Kovács E. Comprehensive study of thiazole-orange-based DNA dyes. ChemPhotoChem. 2024;8:e202400080. doi: 10.1002/cptc.202400080.

Varga N, Pomozi V, Kozák E, Erdei Z, Tóth S, Kutás A, Mucsi Z, Rapi Z, **Kovács B,** Matuscsák A, Bánhídi O, Váradi C, Rácz T, Német K, Viskolcz B, Szepesi Á. Development and validation of combined in vitro and in vivo assays for evaluating the efficacy of strontium-chelating compounds. Sci Rep. 2025;15:43006. doi: 10.1038/s41598-025-06618-1.

10 Acknowledgements

First and foremost, I owe a debt of gratitude to my supervisor, Dániel Hillier. Dani, thank you for the inspiring discussions and the experience of thinking together, where we complemented each other as partners. Thank you for the high expectations and the tough criticism – while there were moments when these were hard to bear, in time I understood that it was all because you saw potential in me and wanted me to be better. I truly learned a great deal from you about science and about myself.

I am incredibly grateful to the members of the Hillier Lab, especially Fanni Somogyi, Klaudia Csikós, Domonkos Horváth, and Ábel Petik – but also to every group member who contributed to this journey. I could not ask for better colleagues. It is hard to put into words the bond we share. You are the kind of colleagues one can always count on, with whom everything can be discussed, and who build rather than destroy. Thank you for listening to all my presentations, for trying to understand what I was working on, and for all your questions and feedback.

I am grateful to Lucia Wittner, who, as the "workplace mom" to us all, was always there when I got stuck, felt disillusioned, or just needed advice.

Special thanks are due to the Co-operative Doctoral Program (KDP), which provided the scholarship that allowed me to focus fully on research, freeing me from the burden of daily livelihood struggles that, unfortunately, so many PhD students have to face. Through this program, I had the opportunity to collaborate with Femtonics Ltd., which offered access to world-class infrastructure and a broad knowledge base. I am grateful to Balázs Rózsa for making this framework and opportunity possible.

Within this program, my corporate expert was Áron Szepesi. I learned a tremendous amount from you about AAVs and cell culture. Although when we first met, you warned me against science and tried to steer me toward floristry instead, I hope that today you look at the result with pride. It meant a lot that I could lean on you personally during difficult moments as well.

From the Femtonics team, special thanks go to Éva Jámbor, who was a stable point throughout my work and helped incredibly much. And I am grateful to Anett Matuscsák: we started developing this project together, and even though I later carried the work forward alone, you were always present in it. Thank you for your continuous interest, for

the times we brainstormed together – sometimes on my scientific questions, sometimes on yours – and for naturally evolving from my "right hand" into a true colleague. Your helpfulness made so many things easier, and your friendship meant even more.
For the essential samples and professional support, I thank Viktória Szabó and Zoltán Zsolt Nagy (Department of Ophthalmology, Semmelweis University). Similar thanks go to Wim Vanduffel (Laboratory for Neuro-and Psychophysiology, Leuven Brain Institute, KULeuven,) and István Hernádi (Grastyán Translational Research Center, and Szentágothai Research Center, Center for Neuroscience, University of Pécs) for providing the macaque samples. I also thank the Cell Biology Unit at the HUN-REN Institute of Experimental Medicine for the use of the Cytation 5 Cell Imaging Multi-Mode Reader.
Finally, I thank everyone – human and animal alike – whose biological samples contributed to these results.

11 Supplementary material

Supplementary Table S1. Dilution strategies in Variable Serum Concentration (VSC) and Constant Serum Concentration (CSC) AAV neutralization assays. *The tables detail the dilution strategies employed in both assay methods. The upper section details the VSC approach, where DMEM serves as the diluent for test serum, resulting in progressively decreasing total serum concentrations across dilutions in the final mixture (from 6.25% to 1.25%). The lower section illustrates the CSC method, where FBS serves as the diluent instead of DMEM, maintaining a consistent 10% total serum concentration across all dilution points in the final mixture. For each assay type, the table shows the precise composition at three stages, using three technical replicates: initial serum dilution, transduction mix preparation (combining diluted serum with AAV), and final concentrations after adding the transduction mix to the cell plate. This approach with matched dilution points (1/4 through 1/256, plus negative control) allows for direct comparison between the two neutralization assay methodologies.*

VSC	Serum dilution			Transduction Mix (serum dilution + AAV Mix)			Cell Plate	Final concentration (Cell Plate + Transduction Mix)		
Serum to test dilution	**DMEM** as diluent	Serum to test	Total serum	DMEM as diluent	Serum to test	Total serum	FBS in medium	**DMEM** as diluent	Serum to test	Total serum
1/4	50.0%	50.0%	50.0%	25.0%	25.0%	25.0%	1.25%	5.00%	5.0%	6.25%
1/8	75.0%	25.0%	25.0%	37.5%	12.5%	12.5%	1.25%	7.50%	2.5%	3.75%
1/16	87.5%	12.5%	12.5%	43.8%	6.3%	6.3%	1.25%	8.75%	1.3%	2.50%
1/32	93.8%	6.3%	6.3%	46.9%	3.1%	3.1%	1.25%	9.38%	0.6%	1.88%
1/64	96.9%	3.1%	3.1%	48.4%	1.6%	1.6%	1.25%	9.69%	0.3%	1.56%
1/128	98.4%	1.6%	1.6%	49.2%	0.8%	0.8%	1.25%	9.84%	0.2%	1.41%
1/256	99.2%	0.8%	0.8%	49.6%	0.4%	0.4%	1.25%	9.92%	0.1%	1.33%
0	100.0%	0.0%	0.0%	50.0%	0.0%	0.0%	1.25%	10.00%	0.0%	1.25%

CSC	Serum dilution			Transduction Mix (serum dilution + AAV Mix)			Cell Plate	Final concentration (Cell Plate + Transduction Mix)		
Serum to test dilution	**FBS** as diluent	Serum to test	Total serum	FBS as diluent	Serum to test	Total serum	FBS in medium	**FBS** as diluent	Serum to test	Total serum
1/4	50.0%	50.0%	100.0%	25.0%	25.0%	50.0%	0%	5.0%	5.0%	10.0%
1/8	75.0%	25.0%	100.0%	37.5%	12.5%	50.0%	0%	7.5%	2.5%	10.0%
1/16	87.5%	12.5%	100.0%	43.8%	6.3%	50.0%	0%	8.8%	1.3%	10.0%
1/32	93.8%	6.3%	100.0%	46.9%	3.1%	50.0%	0%	9.4%	0.6%	10.0%
1/64	96.9%	3.1%	100.0%	48.4%	1.6%	50.0%	0%	9.7%	0.3%	10.0%
1/128	98.4%	1.6%	100.0%	49.2%	0.8%	50.0%	0%	9.8%	0.2%	10.0%
1/256	99.2%	0.8%	100.0%	49.6%	0.4%	50.0%	0%	9.9%	0.1%	10.0%
0	100.0%	0.0%	100.0%	50.0%	0.0%	50.0%	0%	10.0%	0.0%	10.0%

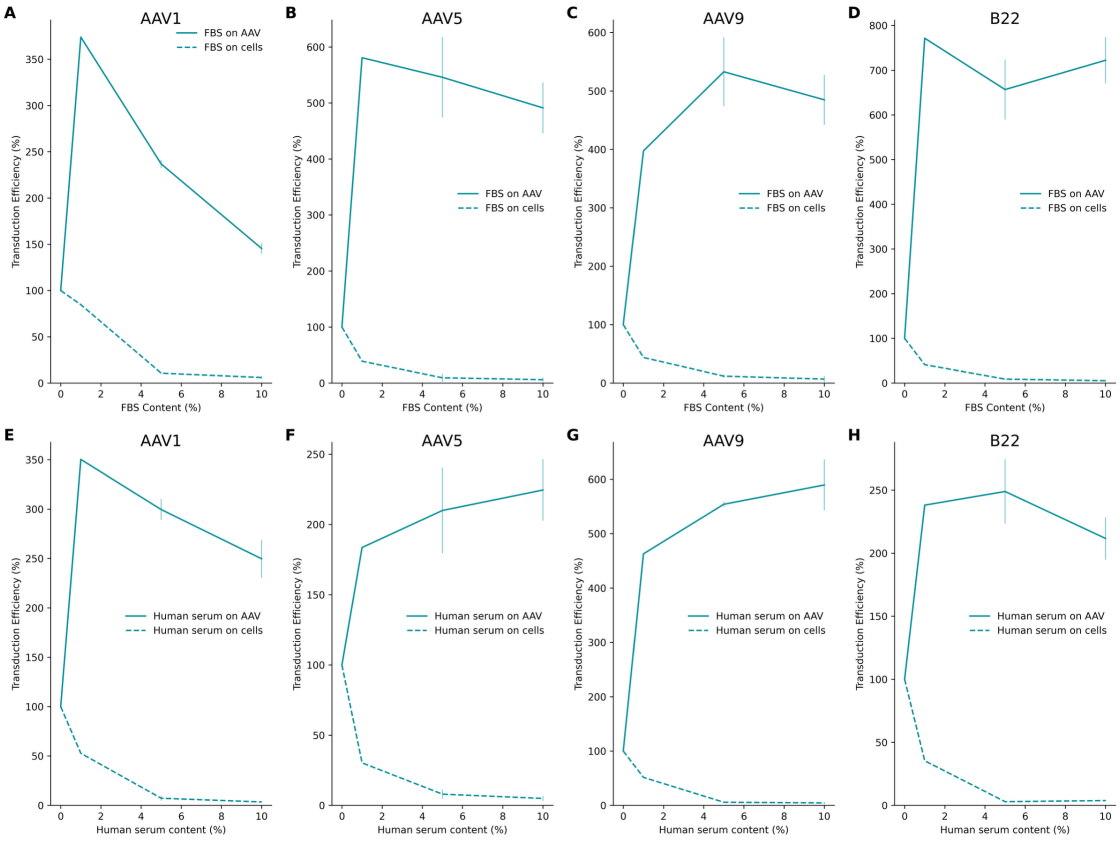

Supplementary Figure S1. Effect of serum content during pre-incubation on transduction efficiency across AAV serotypes and strategies. *Relates to Figure 3. Panels A–D show the effect of fetal bovine serum (FBS) content on transduction efficiency during pre-incubation for AAV1, AAV5, AAV9, and B22 serotypes, respectively. Panels E–H show the effect of human serum content during pre-incubation for the same serotypes. Transduction efficiency was measured 24 hours post-transduction and normalized to the 0% serum condition. The "Serum on AAV" strategy results in a sharp increase in luminescence for both FBS and human serum conditions. In contrast, the "Serum on cells" strategy results in decreased luminescence with increasing serum content across all serotypes. Error bars represent standard deviations.*

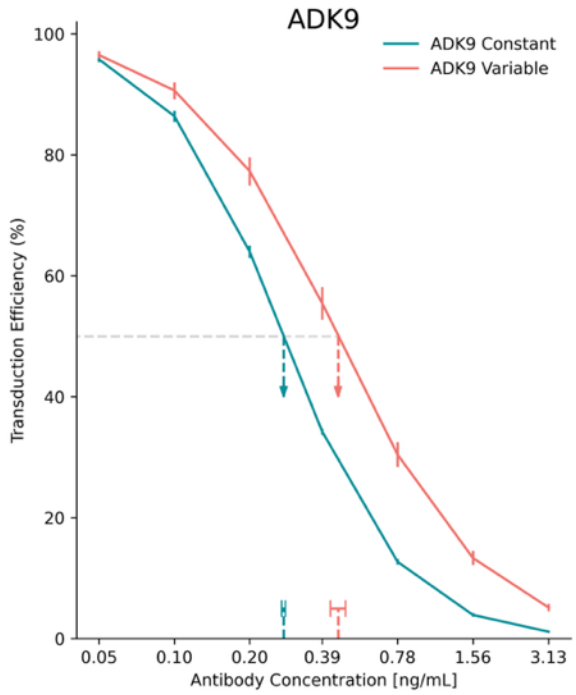

Supplementary Figure S2. Improved sensitivity of ND50 estimation with Constant Serum Concentration (CSC) assay. *Relates to Figure 4H. Neutralization curves obtained from testing ADK9 antibody concentration series with AAV9, via the VSC assay (teal curve) or the CSC assay (orange curve). Vertical error bars denote 95% credible intervals (uncertainty ranges derived from Bayesian analysis), and vertical arrows pointing to horizontal bars denote ND50 estimates along with their uncertainty ranges (Methods).*